8-2013

A Geomechanical Study of the Mississippian Boone Formation

Karen Nicole Mason Buckland
University of Arkansas, Fayetteville

A Geomechanical Study of the Mississippian Boone Formation

A Geomechanical Study of the Mississippian Boone Formation

A thesis submitted in partial fulfillment
of the requirements for the degree of
Master of Science in Geology

By

Karen Nicole Mason Buckland
University of Arkansas
Bachelor of Science in Geology, 2011

August 2013
University of Arkansas

This thesis is approved for recommendation
to the Graduate Council

____
Dr. Gregory Dumond
Thesis Director

____
Dr. Doy Zachry
Committee Member

____

Dr. Phillip Hays
Committee Member

ABSTRACT

The Boone Formation in northwest Arkansas is a chert-limestone sequence analogous to the subsurface Mississippi Lime reservoir in parts of Oklahoma and Kansas. It has low permeability and produces via horizontal drilling and hydraulic fracturing. The response to stimulation by fracturing is dependent on the quantity of chert in the area. Chert nodules and laterally extensive chert layers in the sequence are variable. Locally, cm- to dm-scale chert bedding is continuous and comprises up to 50% of the outcrop. Elsewhere, the chert is nodular and intermittent.

Samples collected from representative outcrops spanning the thickness and aerial extent of the formation are being targeted to establish a geomechanical framework for the reservoir. Samples include end members of chert and limestone and interlayered limestone and chert facies with variable thicknesses and contact geometries. Each sample was cored, confined, and oriented perpendicular to bedding. Compressive strength testing of core plugs were performed to determine the stiffness of the rock, describe how each facies responds to loading and failure, determine how limestone rheology is influenced by the presence of chert, and characterize how rock properties influence the compressive strength of the sample. Rockwell Hardness testing was performed on the samples to understand the strength of the rock in an additional quantitative way.

The compressive strength of the samples and the Rockwell Hardness values of the samples were compared with each other and with the inherent properties of the rock (e.g. lithology, natural fractures, contact types, and facies) to understand and assess correlations and trends in an effort to understand the geomechanics of the Boone Formation.

ACKNOWLEDGEMENTS

Special thanks are due to all of my parents who, by example, taught me work ethic, leadership, independence, and critical thinking. Thank you, James Mason for buying me a geology kit when I was eight and for always encouraging my dreams. You are a great father and the most special man in the world. Thank you, Ava Gail Klesen for not being a stage mom, and for allowing my hard work and abilities to carry me through. Thank you, Linda Mason, for being a free counselor and for treating me like your own. Thank you, Joe Klesen for teaching me a proper handshake. Without your parental guidance, I would not have the skills or the initiative to complete this thesis.

Thank you to Dr. Doy Zachry for being my mentor, for believing in me, and for teaching me almost everything I know about geology.

Thank you to Dr. Greg Dumond for seeing something special in me, for all of your encouragement, and for sharing your enthusiasm for geology.

Thank you to the crew at Stim Lab for generously opening up your facilities to me and for giving your time, sharing your equipment and your resources.

Christy Blair, thank you for your proofreading, presentation critiquing and home-cooked meals. I hope one day to have your style and class. You are my hero!

Thank you to Wanda Meyer and my Gentry family for raising me right and for teaching me how to work and make decisions. I would not be where I am without all of you.

Thank you to my husband, Bill Buckland, for letting me gallivant all over the world, for lending me a shoulder to cry on through the hard classes, for providing me with all the best geology and camping equipment, and for cleaning the litter box when I was gone. I love you!

DEDICATION

This thesis is dedicated to my step-son, William, my nieces, Callie, Hannah, Tori, and Cadie, and my nephews, Chantz, Seth, Tyler, and Brady. I love you all so much. My wish for each of you is that you take every opportunity offered to you on your path to fulfilling your dreams. I hope while you do this you keep an open mind, become comfortable questioning everything, and become confident in all of your opinions. Know that it is okay to develop your own opinions, even if they differ from other people's opinions, including your parent's and your churches'. Have faith in yourself, have faith in God, and know that as long as you are on your correct path in life, you will feel it; I am not saying it will be easy, but you will definitely feel it.. Don't let anyone or anything keep you from fulfilling your dreams because each of you is capable of being anything you set your mind to.

This thesis is also dedicated to me. Karen, this is such an accomplishment, even if it doesn't feel like it right now. This is a time of scary life changes. Please try to know that everything will be okay, and that it is normal to have trepidations. Keep following your path, setting goals, and striving for excellence. Try your best to make it through the next year with a positive attitude. Come out of these new challenges a better person, one you can wholly be proud of in every aspect of life. Use your past to help you make good decisions in the future. Remember the hard times, but don't dwell on them. Use this opportunity to reevaluate and find your true self again. Never forget that attitude is everything, and the rest will fall into place.

TABLE OF CONTENTS

INTRODUCTION

Horizontal drilling and hydraulic fracturing have given the petroleum industry the ability to tap into reservoirs that have not historically been very productive. With older technology, geologists have focused their efforts on shale source rocks to produce natural gas over the last decade. Recently, the petroleum industry has applied these unconventional techniques to carbonate rocks, especially the Mississippian limestone unit located in the subsurface of Oklahoma and Kansas. This carbonate section is inferred to be equivalent to the Boone Formation in northwest Arkansas (Mazzullo et al., 2011), which has extensive subaerial exposure with large outcrops throughout the region. The outcrops in northwest Arkansas have been recognized as an ideal study site that may help the petroleum industry better understand the Mississippian age limestone as a reservoir (Mazzullo et al., 2011).

The Boone limestone has variable porosity and low permeability (Durham, 2013). Petroleum production in the Boone-equivalent unit beneath Osage County in Oklahoma thus requires stimulation by fracturing (Shane Matson, personal communication, 2012). The unit contains chert which is variable in abundance throughout the sequence. In some places, cm- to dm-scale chert beds are continuous and comprise up to 70% of the rock volume. In other places, chert is nodular to intermittent or non-existent. The response to stimulation by hydraulic fracturing is reportedly dependent on the quantity of chert at depth (Shane Matson, personal communication, 2012).

For this thesis, end member samples and mixed lithology samples of limestone, chert, and tripolite in the Boone Formation were taken from multiple key sections within outcrops in the northwest Arkansas region. Unconfined compressive strength tests were performed on oriented cores from each sample, and the behavior of each sample (characterized according to lithology) was described. The relative strength of the lithologies in the Boone Formation was examined and trends in compressive strength, Rockwell Hardness, contact types, fracture density, and facies types were explored in an effort to provide constraints on what to expect during fracturing chert-rich limestone rocks.

II. GEOLOGIC HISTORY

The Mississippian age Boone Formation is the topmost unit of the Springfield Plateau, which encompasses northwest Arkansas, northeast Oklahoma and southwest Missouri as part of the Ozark structural dome (Manger and Evans, 2012). The Lower Mississippian (Osagean) Boone Formation has extensive outcrops in the tri-state area and forms disconformities with Silurian, Devonian, and Ordovician rocks throughout the Springfield Plateau – a part of the Ozark dome (Figure 1).

During the Devonian Period there was significant migration of the North American craton toward the equator and plate collision with the South American plate and intervening island arcs (Blakey, 2009). Convergence continued throughout the Mississippian and Pennsylvanian periods, culminating with the development of the Ouachita thrust front, syn- and post-orogenic development of the Arkoma foreland basin, and regional faulting, fracturing and uplift of the Springfield Plateau by the Permian Period, if not earlier during the Pennsylvanian (Hudson, 2000).

The north central and northwestern parts of Arkansas (Figures 3, 4, and 11) were part of the southern edge of the North American craton during most of the Paleozoic and experienced multiple eustatic cycles during that era (Manger and Evans, 2012). During the Mississippian, the area was part of the passive continental shelf margin (Figure 3 and Figure 4), and rocks correlative with the Boone Formation have been interpreted as forming on the slope of this continental shelf (Gutshick and Sandberg, 1983).

During most the Mississippian period, the Earth was in a first-order greenhouse cycle, where poles were at a glacial minimum, CO_2 production from the mid-ocean ridges was at a maximum, sea level was high, and transgressive waters inundated the North American continent (Smith, 2000). Transgression inundated this region of the North American Craton with water to a depth of about 200 meters, but there were numerous second-, third- and fourth-order regional cycles throughout the Mississippian (Manger and Evans, 2012). These waters were relatively warm and shallow and a variety of organisms inhabited the water. Benthic echinoderms, brachiopods, and bryozoans dominated the seafloor, and many other carbonate-secreting organisms, including planktonic conodonts and nektonic cephalopods also lived in the environment (Gutshick and Sandberg, 1983). Silica-secreting organisms, such as radiolarians and diatoms, also inhabited the shelf environment (Gutschick and Sandberg, 1983).

During the early and middle Pennsylvanian period, the northern advancement of the Ouachita thrust belt due to collision of the Sabine arc terrane caused the formation of peripheral foreland basins along the Mississippian shelf edge due to subsidence, extensional faulting, deposition into and compaction of the Ouachita trough (Sutherland, 1988; Mickus and Keller, 1992). Provenance of the Arkoma Basin indicates prograding fluvial deposits of conglomerate, sand, silt, and clay from the Ouachita thrust belt, terrigenous clastics from the North American craton, and some sediment from the eastern Black Warrior Basin (Sutherland, 1988). The weight of the Ouachita thrust sheets, flexural downwarping of the Arkoma Basin, and bending of the North American plate margin during south-directed subduction caused uplift of the Ozark Dome (Hudson, 2000; Stoffell et al., 2008). Although the exact timing of the uplift is unknown, there is no evidence of Permian rocks in the Ozark Dome, nor unconformities with younger age rock units. This suggests that much of the uplift may have occurred during the late Pennsylvanian (Hudson, 2000). This uplift contributed to the end of deposition in the area and the lithification, exposure, faulting and uplift of the Springfield Plateau, the area of interest for this thesis. Mississippian age rocks comprise the topmost unit of the Springfield Plateau, which encompasses the tri-state area of Arkansas, Oklahoma, and Missouri (Figure 1)

III. ROCK UNIT DESCRIPTION

The rock unit of interest for this thesis is the Boone Formation. As previously discussed, it is interpreted as a carbonate platform/slope/shelf deposit that has been exposed by regression, uplift, and erosion. Due to diagenesis, the current physical and chemical properties of the Boone Formation are different than when the unit was first formed. During deposition, the Mississippian platform/slope/shelf would have consisted of relatively pure limestone with interbedded micrites, and fossils with intermittent deposition of clay and sand (Gutschick and Sandberg, 1983).

Over geologic time, however, there has been significant chemical and erosional alteration of the Boone Formation (Rogers, 2001). The outcrops in the Springfield Plateau show the lithological complexity of the Boone Formation. In outcrop and in the subsurface, the Boone Formation has repeating sequences of limestone and chert of variable thickness. The Boone Formation varies in thickness from 300 to 390 feet (McFarland, 2004). Clay and shale are not uncommon in the Boone Formation. In some places, calcareous fossils are preserved by silica replacement. In other places, the fossiliferous nature of the Boone Formation is expressed by negative imprints, where the fossils were not replaced by silica and have undergone dissolution leaving only the impression of the outside of the hard parts of the animal.

Samples for this thesis were taken from localities in Arkansas, Oklahoma and Missouri. All the sites are Lower Mississippian (Osagean) limestone/chert outcrops, however, when crossing state lines the nomenclature of the units change. As stated above, the Arkansas nomenclature of the unit of interest is the Boone Formation. In Oklahoma and Missouri the unit name is the Reeds Spring (Figure 10). This thesis will refer to the unit as the Boone Formation, as the majority of samples were from Arkansas. There was one sampling site each from Oklahoma and Missouri, and both were within 10 miles of the Arkansas state line (Figure 2).

For the purpose of this thesis, the Boone Formation has been divided into four stratigraphic facies with variable chert, tripolite, and limestone associations (Figure 6). This division is based on the slope model of Gutshick and Sandberg (1983) as shown in Figure 5 and assumes transportation of material down the slope. Downslope transportation is inferred to have caused the lobate geometry seen in outcrop (Figure 7) and explains the basinward transport of platform organisms also seen in outcrop (Doy Zachry and Walter Manger, personal communication, University of Arkansas, 2012).

The bottom most unit of the Boone Formation will be considered Facies 1. Facies 1 is distinct in that it has dark blue, black and dark gray chert nodules and dark gray limestone. The chert in Facies 1 is nodular, and the limestone appears lobate and “squeezed in between” the chert nodules. Based on the dark color and the location, Facies 1 is inferred to represent the toe of the foreslope and the inflection point of the slope and the basin on the Gutshick and Sandberg (1983) model.

Facies 2 is above Facies 1, and Facies 2 has light blue and light gray chert and medium gray limestone. The chert and limestone define bedding planes in Facies 2. Facies 2 represents the lower half of the slope on the Gutshick and Sandberg (1983) model.

Facies 3 overlies Facies 2 and underlies Facies 4. Facies 3 is characterized by bleached white chert and light gray chert with light gray limestone. Facies 3 chert and limestone intervals also follow the bedding planes, and the chert is more prevalent than the limestone. Facies 3 approximately coincides with the upper half of the slope on the Gutshick and Sandberg (1983) model.

Facies 4 is the topmost unit of the Boone Formation. Facies 4 is characterized by tripolite (altered limestone) and light gray to medium brown limestone. Facies 4 is found at the top of the outcrops of the Boone, but it can vary in thickness from site to site. The chert/limestone intervals in Facies 4 are long and continuous following bedding planes. There is significantly more tripolite than limestone in this facies. Facies 4 is inferred to represent the area around the inflection point between the platform and the foreslope on the Gutshick and Sandberg (1983) model.

The two types of chert in the Boone Formation, bedded and nodular, indicate that the silica for chert formation may have different sources and depositional timing. The nodular chert (Figure 8), found as the basin/slope inflection point, has been interpreted as being deposited penecontemporaneously (Walter Manger, personal communication, University of Arkansas, 2012). The lack of bedding planes and the presence of “squeezed” limestone in Facies 1 indicates that the chert was formed prior to induration and compaction. The chert in Facies 2-4 (Figure 9) follows the bedding planes of the limestone and tends to be lighter in color, which may indicate that silica replacement in these portions of the Boone Formation occurred after induration by silica-rich groundwater (Manger et al., 2002; Manger and Evans, 2012; Doy Zachry, personal communication, University of Arkansas, 2012).

The Mississippian Lime outcrops in Arkansas, Oklahoma and Missouri, but in each state is recognized by different nomenclature. Figure 10 shows a stratigraphic column of Mississippian age rocks for each state for reference.

IV. BACKGROUND

Rock mechanics refers to the way that a rock's physical properties affect the rock's mechanical response to stress and strain. Fracture development in rocks is one aspect of rock mechanics, and fracture propagation can range from the microscopic level to a magnitude of several kilometers (Pande et al., 1990). Natural fractures in the Boone Formation outcrops span across the entire rock mechanics scale. Fractures in the rock samples for this study range from fractions of millimeters to approximately 1/3 meter; fractures in the individual outcrops can be up to hundreds of meters; fractures across the entirety of the Boone Formation are on the order of 10s of kilometers, coinciding with the NE-trending faults in northwest Arkansas (e.g., Hudson, 2000). The Boone Formation has undergone a significant amount of diagenesis and many of the natural fractures are mineralized. Calcite is the primary mineral in the fractures, but quartz, dolomite, chalcopyrite, sphalerite, and pyrite are present in some fractures (Leach and Rowan, 1986). In order to understand the inherent geomechanical properties of a rock, lab testing can be done on samples from both outcrops and subsurface rock. The resulting data can be used to predict how rocks will behave in different situations (Coates, 1970). Rock mechanics has a wide array of applications in the fields of civil engineering and geology. In engineering, rock mechanics is particularly useful in the building of structures, dams, and the infrastructure required in the modern world (Jumikis,1979). Specifically, rock properties would help engineers model how bedrock and structures would behave in an earthquake, how strong bridges and roads need to be to accommodate traffic, and how much water pressure a dam can safely sustain. Geological applications of rock mechanics include, but are not limited to, quarrying, mining, and hydraulic fracturing in petroleum reservoirs. Knowledge of rock properties allows geologists to model the appropriate water pressure or blasting pressure needed to cut out rocks to build roads, to safely make tunnels, and to excavate solid, liquid, and gaseous resources. The excavation of liquid and gaseous resources is done in a wellbore using a technique called hydraulic fracturing.

Hydraulic fracturing (also known as fluid stimulation: Pettitt, 2011) is used to induce higher flow of oil or natural gas from a reservoir to a production well. After a well is drilled, a mixture (often company-specific) of water, chemicals, and sand-sized particles under pressure is injected down the borehole to a portion of the well that is isolated. The hydraulic pressure is increased until the point where the tensile strength of the rocks is overcome, causing fractures to propagate into the reservoir rock at the isolated interval (Jumikis, 1979). These fractures are held open by particles in the solution, known as proppant, which facilitate greater permeability and flow of liquid or gas through the rock. Increases in the productivity of the well are proportional to the increase in the permeability of the rock, which is based on the width, length, and intricacy of the fracture network created by hydraulic fracturing (Ameen et al., 2012).

The pressure induced by hydraulic fracturing causes tensile stress on the rock (Jumikis, 1979), however, tensile strength testing equipment was not available for use for with this thesis; unconfined compressive failure tests on sample plugs were performed instead. In an unconfined compressive strength test, a cylindrical plug core is put under a constant load to the point of failure. At the failure point, the rock will fail across its long axis, undergo splitting, or experience shear failure (Jumikis, 1979).

Hydraulic fracturing is closely related to rock mechanics in that 1) in order to fracture the rock, the mechanical properties of that rock must be known, and 2) the magnitude of the fractures needed for a particular unit will vary, so computations based on rock mechanics of the unit are necessary. Despite significant mineral infilling, the natural fractures in the Boone Formation may make it a good reservoir in the subsurface and hydraulic fracturing would enhance the conductivity of the oil through the fractures during production, as observed in the Mississippi Lime reservoir in Osage County, Oklahoma (Shane Matson, personal communication, Spy Glass Energy, 2012).

The Mississippi Lime Play is an oil and gas play in the subsurface of north central Oklahoma, south central Kansas and northwest Kansas. Production from the Mississippi Lime Play comes from both the chert/limestone facies and the tripolite facies. The chert/limestone facies forms a reservoir from the porosity of abundant natural fractures in the chert and the limestone forms seals for the reservoir (Mazzulo et al., 2011). Because the amount of chert and location of chert are variable throughout the unit, reservoirs within this facies of the Mississippian are abundant, but have sporadic depths and aerial extents (Matson, 2011). The tripolite section forms a reservoir from secondary porosity. This secondary porosity forms during from the alteration of the chert to tripolite in which the remnant limestone (microscopic size portions of the original limestone and carbonate fossils that did not get replaced by silica during diagenesis) weathers out of the rock, leaving voids in the rock and causing the primary component of the rock to become silica (Mazzullo et al., 2011 and Doy Zachry, personal communication, University of Arkansas, 2012) The tripolite referred to as the Pineville tripolite facies in Missouri, where is the most abundant in outcrop.

There are five active chert reservoirs in North America including the Mississippi Lime Play of the Cherokee Platform of Oklahoma. The other four are the Thirtyone Formation in the Permian Basin of West Texas, the Monterey Formation of the San Joaquin Basin in California, the Wabamun Formation of the Western Canada Basin, and the Amsden Formation of central Montana.

The Thirtyone Formation is a Devonian age unit with two lithofacies of chert. 1) a thick diagenetic chert controlled by faults and fractures, inferred as a proximal ramp setting, and 2) a series of stacked, thin laminated cherts, mixed with burrowed cherts and spicule dominated skeletal packstones ,inferred as a distal ramp setting (Ruppel, 2005). This reservoir is sourced from the overlying Woodford Shale unit, has porosity estimates as high as 25% and permeability estimated at 5-20 md. This unit is expected to produce 1400 million barrels of oil (Ruppel and Barnaby, 2001).

The Monterey Formation is a Miocene age unit consisting of interbedded chert and shale layers. The chert both nodular and bedding plane controlled. This chert is classified as porcelainite. The silica and porosity are derived from the dehydration of opal (55-60% porosity) and the dissolution of diatoms(10-20% porosity). This reservoir has expected production of one million barrels of oil. (Reid and McIntyre, 2001)

The Wabamun Formation a dolomitized carbonate unit capped by a 100 foot thick section of replacement chert attributed to precipitation from a hydrothermal source. This is a natural gas reservoir with 225 bcf of expected production. The Wabamun Formation is a fault controlled reservoir with porosity in the chert of up to 30%. This porosity is formed in the space between the microintercrystalline quartz prisms, and tight limestones serve as seals for the reservoir (Packard et al., 2001)

The Amsden Formation is a Pennsylvanian unite found in the Wolf Springs field of Montana. This unit consists of chert breccias and dolomite clasts. This unit is associated with dissolution, karsting, and collapse of evaporate deposits. As of 2001, the Wolf Springs field produced 5.7 million barrels of oil, mostly from the Amsden Formation (Luebking et al., 2001)

V. METHODOLOGY

For this thesis, five representative outcrops in the Mississippian portion of the Springfield Plateau were selected (Figure 2), and numerous samples of chert, limestone, tripolite and interlayered chert, tripolite, and limestone with variable thicknesses and contact geometries were collected from each outcrop. Photos can be found in the appendix. These samples were taken to Stim Lab, a division of Core Lab in Duncan, Oklahoma. At Stim Lab, a 20-inch diameter diamond-tipped saw was used to cut a ½ inch slab from each sample. Thirty-five slabs were made in total. The remaining portion of each hand sample was then cored perpendicular to bedding using a stationary drill press and diamond-imbedded coring bit with a 1-inch diameter. Not all the hand samples remained intact during the coring process; therefore, only a subset of samples was successfully cored. Of the twenty-six samples that were successfully cored, only two cores had lengths greater than 1 inch. The cores were then faced (i.e., cut precisely) on each end using a 6-inch diameter diamond-imbedded blade. Photos of the cores can be found in the appendix. Two geomechanical tests were performed: uniaxial compressive strength tests on the plugs and Rockwell Hardness tests on the slabs.

The plugs were photographed and measured for diameter and length prior to being placed into an unconfined uniaxial compression rig. Once positioned in the machine, a constant compressive stress at a rate of 1000 pounds square inch (psi)/minute was applied to each plug to the point of brittle fracture and failure. Data was recorded directly from the machine to a computer and includes the stress (in psi) applied and the time of failure at the breaking point. The maximum stress recorded prior to the breaking point is analogous to the ultimate strength (S) of the samples during the experiment. The maximum load applied (P) at the time of failure was hand recorded from the machine. For each sample run, the strength (S) was plotted against time (t). The individual graphs are shown in the Appendix section of this paper, and Figure 12 is a consolidated graph of all the runs. The procedures for the compression test follow ASTM International Designation D 2983-95 (2002). ASTM International Designation D 4543-08 specifies how the core for the compressive stress testing should be prepared. However, due to the natural fractures and brittle rheology of the samples, some modifications to the typical procedures were implemented. These modifications included: 1) the plugs had a diameter of 1inch instead of the typical 1 and 7/8 inches, and 2) the plugs were generally about 1 inch in length instead of the typical length required to be 2 to 2 and 1/2 times the diameter. These modifications are typical of rock mechanic studies for unconventional reservoirs (Mike Conway, personal communication, Core Lab, CEO Stim Lab Division, 2012).

A Service Diamond hardness tester (model #8BLP) was used to determine the Rockwell Hardness value of the limestone and chert in each slab. Conforming to Rockwell Hardness Scale H, the indention tool was loaded with a 1/8-inch ball and the major load was set to 60 pounds. Each ½-inch slab was loaded into the Service Diamond machine and tested separately. The slab was positioned such that the indention tool was set over the limestone portion of the slab. The minor load of 10 kilograms-force (kgf) was applied by pulling the lever on the right forward and rotating the platform up to tighten the slab into the indention tool. The platform was rotated upward until the minor load was set. This was followed by application of the major load of 60 kgf. When application of the load stopped (or slowed significantly to within 45 seconds), the value was recorded to the nearest 0.25, and this value represents the indentation value. The load was released and the value was recorded a second time, representing the Rockwell Hardness Number. The slab was then adjusted so that another point on the limestone could be measured. This procedure was done eight times for the limestone portion of the slab, and the procedure was repeated eight times on several chert portions of the slab. An average limestone Rockwell Hardness Number and an average chert Rockwell Hardness Number were calculated from the eight runs. The entire procedure was repeated for each of the samples; however, in the cases where the sample only had one lithology, only one series of testing was done. These procedures follow the ASTM International E18-08b guidelines, but the averaging process was a modification implemented due to the nature of the rock and due to the use of the hardness tester on anisotropic rock instead of isotropic metal - the machine's intended experimental material.

VI. RESULTS

Figure 12 shows the range of brittle compressive strength for 26 samples. The psi (pounds per square inch) values range from a low of 778.4 psi for sample KB-4A to a high of 8370 psi for sample KB-2i.

By weighted average, the range of Rockwell Hardness values is from a low of H46.7 for sample KB-5A to a high of H95.4 for sample KB-5A. Figure 13 displays a line graph of Rockwell Hardness values by chert, limestone, and tripolite respectively. Chert values plot higher than the limestone. Tripolite values plot lower than limestone.

Sorting by the percentage of chert in the sample (Table 2) illustrates that the samples with less than 50% chert content primarily have sharp contact types and samples with more than 70% chert favor diffuse contact types (Figure 14). The end-members of chert, limestone, and tripolite all have a relatively low number of fractures. The samples that do not contain chert have the lowest average Rockwell Hardness at H74 (Figure 16) and the lowest average compressive strength at 2675.3 psi (Figure 15). Samples that contain 20%-50% chert have an average Rockwell Hardness of H83.1and an average compressive strength of 2950.2. Samples with 70%-100% chert have the highest average Rockwell Hardness of H84.9 and the highest compressive strength at 3492.8 psi.

Sorting by percentage of limestone (Table 3) shows that the samples comprised of less than 20% limestone have a low fracture density (Figure 17) and diffuse contact zones. These samples have the highest compressive strength average at 4769.4 psi (Figure 18) and the second highest Rockwell Hardness average at H82.4. The range of 20%-50% limestone composition yields the highest Rockwell Hardness average of this group at H83.6 and the lowest compressive strength of the group at 2367.8 psi. The samples that contain 50%-100% of limestone have the lowest Rockwell Hardness of the group at H80.2 and the mid-range compressive stress at 2961.2 psi.

Sorting by the percentage of tripolite (Table 4) indicates that the sampling range of the tripolite was not as variable as the other two compositions. The 20%-50% range produces the lowest Rockwell Hardness average of H66.1 and the highest compressive strength average at 3200.1 psi (Figure 19). The division that contains greater than 50% tripolite has the lowest compressive strength at 2564.7 psi and the middle Rockwell Hardness average at H72.8. The highest Rockwell Hardness average belongs to the category with less than 20% tripolite.

A sort by the facies division produces a trend in in fracture amount and in compressive strength (Table 5). Facies 1 and Facies 2 have trends of moderate to abundant fracture density (Figure 20). Facies 3 and Facies 4 have relatively fewer fractures. The average compressive strength value for each facies increases from Facies 1, with 2843.8 psi, through Facies 4, with 3347 psi (Figure 21). Facies 2 has the highest Rockwell Hardness average at H90.9 and Facies 4 has the lowest Rockwell Hardness average at H76.9 (Figure 22).

Sorting by fracture amount (Table 6) illustrates that the samples with low fracture density (1%-25%) are primarily from Facies 3 and Facies 4. The samples with medium (25%-50%) and high (50% or more) fracture densities are primarily from Facies 1 and Facies 2. The two lowest compressive strength values fall into the high fracture density group, and the 2 highest compressive strength values fall into the low fracture density group (Figure 23). The samples with no fractures have both the lowest Rockwell Hardness average, at H67.3 (Figure 24) and the lowest average compressive strength at 1850.2 psi. The samples with medium fracture density amounts have the highest Rockwell Hardness average, at H90.8. The samples with low fracture density amounts have the highest compressive stress average at 3668.7 psi.

When the data is sorted by contact type (Table 7), Facies 3 is dominated by diffuse contact type. The three highest and the two lowest compressive strength values have diffuse contact types; these also have the highest compressive strength average at 3492.1 psi (Figure 25). The samples with no contact zones have the lowest overall Rockwell Hardness average at H78.5 (Figure 26) and the lowest compressive strength average at 2663.8 psi. The Rockwell Hardness value averages for the diffuse and the sharp contact types are H85.9 and H82.6 respectively.

A Rockwell Hardness value sort (Table 8) indicates that all of the values below H80 have fracture densities less than 25%, and all but one of these samples is from Facies 3 or Facies 4.

The highest Rockwell Hardness values range from H89.3 to H95.4. All but one of the samples in this series have more than 50% chert. The outlier has 90% tripolite. The lowest Rockwell Hardness values of H71.6 and below are dominated by limestone + chert lithologies that contain at least 40% tripolite. The 2 exceptions are the lowest value of H46.7, which is a graded fossiliferous limestone and a bleached chert from Facies 3. The midrange of Rockwell Hardness values is primarily composed of samples with limestone components higher than 50%.

Sorting by compressive strength (Table 9) shows that the weakest sample (Figure 28), with a strength of 778.4 psi, is a sample with 70% chert and 30% limestone from Facies 3; it has abundant fractures and diffuse contacts, with a Rockwell Hardness of H91.1. The strongest sample, with a value of 8370 psi, is also from Facies 3, but has 95% chert and 5% limestone; it has low fracture density and diffuse contacts, with a Rockwell Hardness of H87. The second weakest sample, with a value of 1054.9 psi, has 80% chert and 20% limestone and is from Facies 2. It has abundant fractures, diffuse contacts, and has a Rockwell Hardness of H91.1. The second strongest sample, with strength of 6353.1 psi, has 97% chert and 3% limestone and is from Facies 3. It has low fracture density, diffuse contacts, and a Rockwell Hardness of H89.3

VII. DISSCUSSION AND INTERPRETATION

The trends in the data for this project become more apparent when the different factors and variables are grouped together, sorted, and averaged. This discussion is heavily based on those averages, and the averages can be seen in each table.

The proliferation of fractures in the chert of Facies 1 and 2 compared to Facies 3 and 4 is indicative of the lithology of the rocks. Where there are more fractures, the chert is more brittle, and the decrease in the amount of fractures in the tripolite facies and bleached chert facies suggest that as alteration of the chert ensues, the fractures that were likely once a part of the rock have become indistinguishable from the pore space left by the weathering of the limestone. Facies 1 and 2 are more brittle and have abundance in fractures, thus they have average compressive strengths that are significantly lower than Facies 3 and 4. From the data, it appears that fracture amount is more of a controlling factor for compressive strength than amount of pore space because Facies 4, the tripolite facies with large pore space volume, has a higher compressive strength than facies with unaltered chert and heavy fractures.

The contact type is controlled by lithology and does not seem to be a controlling factor for compressive strength or Rockwell Hardness values.

Comparing and contrasting the samples with the lowest (sample KB-4A with 778.4 psi) and highest (sample KB-2i at 8370 psi) compressive strengths reveals that they are similar in that they are both from Facies 3 and have diffuse contact types. The key differences between the two samples are 1) the amount of chert and 2) the amount of fractures. The weaker sample has a 30% lower amount of chert and approximately twice as many fractures. This observation would lend itself to the conclusion that percent chert and amount of fractures are the main controlling factors for compressive strength, however, when looking at the overall trend of the percent chert across the samples, it becomes apparent the percent chert and the compressive strength do not correlate. The samples with a high percentage of fractures do form a trend in lower compressive strength values (Figure 23).

The graph of the Rockwell Hardness values (Figure 13) shows that there is a discernible difference between the hardness values of the chert and limestone. The chert trend line is higher than the limestone trend line. This would be explained by the mineralogical differences in the two rocks. The chert has a high silica content and the limestone has a high calcite content. The mineralogical structure of the chert is known to have a higher hardness value than the calcite on the Moh's Hardness Scale, so it would follow that the same would be true for other hardness scales as well. This experiment confirms that assessment. However, the tripolite samples show hardness values that range from lower than the limestone to as high as the chert. This variation could be explained by the amount of alteration each sample of tripolite has undergone. Thin section petrology and a greater sampling range would be needed to determine the empirical differences in alteration of the samples, but from this data it appears that the samples that have undergone the most alteration, and have the higher amounts of tripolite and lower amounts of chert, have the highest Rockwell Hardness values of the tripolite dataset. The explanation that best fits this is that as the limestone weathers out of the chert and leaves remnant silica, the silica produces a higher Rockwell Hardness value because there is less limestone to soften the sample. However, some of the tripolite samples have Rockwell Hardness values less than the limestone samples. Again, this would have to be determined on a microscopic level, but amount of pore space, amount of calcite infilling, and propensity to fracture are likely important variables that would contribute to the variation in the tripolite Rockwell Hardness values.

There appears to be very little direct correlation between the Rockwell Hardness values and the compressive strength values (Figure 27). It was proposed in the background section of this thesis that it could be expected that the samples with higher Rockwell Hardness values would be more brittle and would therefore have lower compressive strength values and that the samples with lower Rockwell Hardness values would be more ductile and would therefore have higher compressive strength values. The compressive strength tests were not controlled well enough to make that comparison and the data does not support the hypothesis. However, the data shows that on average both the compressive strength and the Rockwell Hardness values increase as the percent of chert in the rock increases (Table 2 and Figures 15 and 16).

IX. CONCLUSION

There are three main differences between the samples with the lowest and highest compressive strengths: percent of chert, Rockwell Hardness value, and amount of fractures. There is a trend across the sample dataset that supports that the amount of chert has a strong controlling factor over the compressive strength of the rocks based on average compressive strength results. A high Rockwell Hardness end member corresponds to the low compressive strength value and a lower Rockwell Hardness value corresponds to the high compressive strength end member, however, neither of these Rockwell Hardness values are an end member in their category and there is not a trend suggesting that the Rockwell Hardness values correlate with the compressive strength values of the samples. The fracture amount appears to have a moderate effect on the compressive strength and a slight trend suggests that the samples with more fractures have a lower compressive strength than those with fewer fractures. However, based on this data, there is not a strong enough case to suggest that any of these factors are a primary controlling factor for compressive strength across the Boone Formation. These inconclusive results are likely a product of random sampling and an inability to produce sample plugs of regulatory length. There is also a possibility, because the samples were all taken from a quarry or road cuts, that blasting affected the inherent property of the rocks and skewed some of the results. There would be some merit in obtaining well core, performing the same type of experiment and comparing the results.

The Rockwell Hardness values are clearly controlled by lithology. For this set of samples, there are clear trendlines for the silica-rich chert and the calcite-rich limestone, but the tripolite samples, in varying stages of alteration, do not indicate a trend. It is possible that a petrological study of the tripolite in thin section could explain the variation in hardness, but that is outside the scope of this project.

Overall, when viewing this dataset in sorted property groups and averages, some important trends stand out. Most notably, the percent of chert has some control over compressive strength, Facies 3 is the strongest, the greater amount of fractures in a chert lithology yield a lower compressive strength, and vertical fractures appear to produce a greater resistance to brittle failure. However, without grouping and averaging trends, none of these results are nearly as evident. A more methodological sampling process and more advanced testing equipment could enhance the constraints on the data and provide more conclusive results.

X. TABLES

Table 1. Sort by sample #

Sample#	Sample Name	Run #	% Chert Slab	% LS Slab	% Trip Slab	Facies	Contact	Frac Amt	RWH Avg	PSI
1	KB 2F	1	0.8	0.2	0	2	Diffuse	4 Heavy	91.12	1054.90
2	KB 4F	2	0.5	0.5	0	1	Sharp	3 Medium	95.05	2939.60
5	KB 4B	3	0	1	0	3	None	2 Light	80.3	2007.70
7	KB 1B	4	0.5	0.5	0	2	Sharp	4 Heavy	86.65	3088.30
8	KB 1C	5	0.4	0.6	0	3	Sharp	2 Light	85.78	2513.30
9	KB 4D	6	0.25	0.75	0	1	Diffuse	4 Heavy	86.65	2202.70
10	KB 5A	7	0	1	0	2	None	2 Light	95.4	3617.00
11	KB 2A	8	0.8	0.2	0	1	Sharp	4 Heavy	94.48	3687.50
13	KB 3A	9	0	1	0	4	None	4 Heavy	82.4	3541.00
14	KB 2B	10	0	0.85	0.15	4	Sharp	2 Light	87.655	3058.50
16	KB 1D	11	0.2	0.8	0	1	Sharp	3 Medium	86.64	4124.80
20	KB 1E	12	0.75	0.25	0	2	Sharp	3 Medium	95.2	2013.20
21	KB 5C	13	0	0.35	0.65	4	Sharp	2 Light	68.74	1445.90
22	KB 2E	14	0.85	0.15	0	3	Diffuse	2 Light	72.5	4251.50
24	KB 2G	15	0.4	0.6	0	2	Sharp	3 Medium	86.32	4017.90
25	KB 2K	16	0.9	0.1	0	3	Diffuse	1 None	75.33	1983.50
26	KB 3E	17	0	1	0	1	None	1 None	46.7	1264.20
27	KB 2J	18	0.8	0.2	0	3	Diffuse	2 Light	68.48	2942.90
28	KB 5D	19	0	0.55	0.45	4	Sharp	2 Light	60.635	4097.30
29	KB 4A	20	0.7	0.3	0	3	Diffuse	4 Heavy	91.1	778.40
30	KB 2I	21	0.95	0.05	0	3	Diffuse	2 Light	86.975	8370.00
31	KB 5E	22	0	0	1	4	None	2 Light	87.8	2888.90
32	KB 2H	23	0	0.35	0.65	4	Sharp	2 Light	61.95	3359.20
33	KB 1F	24	0	0.6	0.4	4	Sharp	1 None	71.6	2302.90
34	KB 5F	25	0.97	0.03	0	3	Diffuse	2 Light	89.3	6353.10
35	KB 5G	26	0	0.9	0.1	4	Sharp	2 Light	92.5	2787.60

Table 2. Sort by % Chert

Sample#	Sample	Name	Run #	% Chert Slab	% LS Slab	% Trip Slab	Facies	Contact	Frac Amt	RWH Avg	PSI
31	KB	5E	22	0	0	1	4	None	2 Light	87.80	2888.90
35	KB	5G	26	0	0.1	0.9	4	Sharp	2 Light	92.50	2787.60
21	KB	5C	13	0	0.35	0.65	4	Sharp	1 Light	68.74	1445.90
32	KB	2H	23	0	0.35	0.65	4	Sharp	2 Light	61.95	3359.20
28	KB	5D	19	0	0.55	0.45	4	Sharp	2 Light	60.64	4097.30
33	KB	1F	24	0	0.6	0.4	4	Sharp	1 None	71.60	2302.90
5	KB	4B	3	0	1	0	3	None	2 Light	80.30	2007.70
13	KB	3A	9	0	1	0	4	None	4 Heavy	82.40	3541.00
26	KB	3E	17	0	1	0	1	None	1 None	46.70	1264.20
14	KB	2B	10	0	0.85	0.15	4	Sharp	2 Light	87.66	3058.50
Avg.										74.03	2675.32
16	KB	1D	11	0.2	0.8	0	1	Sharp	3 Medium	86.64	4124.80
9	KB	4D	6	0.25	0.75	0	1	Diffuse	4 Heavy	86.65	2202.70
8	KB	1C	5	0.4	0.6	0	3	Sharp	2 Light	85.78	2513.30
24	KB	2G	15	0.4	0.6	0	2	Sharp	3 Medium	86.32	4017.90
10	KB	5A	7	0.5	0.5	0	2	None	2 Light	95.40	3617.00
2	KB	4F	2	0.5	0.5	0	1	Sharp	3 Medium	95.05	2939.60
7	KB	1B	4	0.5	0.5	0	2	Sharp	4 Heavy	86.65	3088.30
Avg.										83.09	2950.16
29	KB	4A	20	0.7	0.3	0	3	Diffuse	4 Heavy	91.10	778.40
20	KB	1E	12	0.75	0.25	0	2	Sharp	3 Medium	95.20	2013.20
1	KB	2F	1	0.8	0.2	0	2	Diffuse	4 Heavy	91.12	1054.90
11	KB	2A	8	0.8	0.2	0	1	Sharp	4 Heavy	94.48	3687.50
27	KB	2J	18	0.8	0.2	0	3	Diffuse	2 Light	68.48	2942.90
22	KB	2E	14	0.85	0.15	0	3	Diffuse	2 Light	72.50	4251.50
25	KB	2K	16	0.9	0.1	0	3	Diffuse	1 None	75.33	1983.50
30	KB	2I	21	0.95	0.05	0	3	Diffuse	2 Light	86.98	8370.00
34	KB	5F	25	0.97	0.03	0	3	Diffuse	2 Light	89.30	6353.10
Avg.										80.22	3367.76

Table 3. Sort by % Limestone

Sample#	Sample Name	Run #	% Chert Slab	% LS Slab	% Trip Slab	Facies	Contact	Frac Amt	RWH Avg	PSI
31	KB 5E	22	0	0	1	4	None	2 Light	87.80	2888.90
34	KB 5F	25	0.97	0.03	0	3	Diffuse	2 Light	89.30	6353.10
30	KB 2I	21	0.95	0.05	0	3	Diffuse	2 Light	86.98	8370.00
25	KB 2K	16	0.9	0.1	0	3	Diffuse	1 None	75.33	1983.50
22	KB 2E	14	0.85	0.15	0	3	Diffuse	2 Light	72.50	4251.50
Avg.									82.38	4769.40
1	KB 2F	1	0.8	0.2	0	2	Diffuse	4 Heavy	91.12	1054.90
11	KB 2A	8	0.8	0.2	0	1	Sharp	4 Heavy	94.48	3687.50
27	KB 2J	18	0.8	0.2	0	3	Diffuse	2 Light	68.48	2942.90
20	KB 1E	12	0.75	0.25	0	2	Sharp	3 Medium	95.20	2013.20
29	KB 4A	20	0.7	0.3	0	3	Diffuse	4 Heavy	91.10	778.40
21	KB 5C	13	0	0.35	0.65	4	Sharp	2 Light	68.74	1445.90
32	KB 2H	23	0	0.35	0.65	4	Sharp	2 Light	61.95	3359.20
7	KB 1B	4	0.5	0.5	0	2	Sharp	4 Heavy	86.65	3088.30
2	KB 4F	2	0.5	0.5	0	1	Sharp	3 Medium	95.05	2939.60
Avg.									83.64	2367.77
28	KB 5D	19	0	0.55	0.45	4	Sharp	2 Light	60.64	4097.30
33	KB 1F	24	0	0.6	0.4	4	Sharp	1 None	71.60	2302.90
8	KB 1C	5	0.4	0.6	0	3	Sharp	2 Light	85.78	2513.30
24	KB 2G	15	0.4	0.6	0	2	Sharp	3 Medium	86.32	4017.90
9	KB 4D	6	0.25	0.75	0	1	Diffuse	4 Heavy	86.65	2202.70
16	KB 1D	11	0.2	0.8	0	1	Sharp	3 Medium	86.64	4124.80
14	KB 2B	10	0	0.85	0.15	4	Sharp	2 Light	87.66	3058.50
35	KB 5G	26	0	0.9	0.1	4	Sharp	2 Light	92.50	2787.60
26	KB 3E	17	0	1	0	1	None	1 None	46.70	1264.20
5	KB 4B	3	0	1	0	3	None	2 Light	80.30	2007.70
13	KB 3A	9	0	1	0	4	None	4 Heavy	82.40	3541.00
10	KB 5A	7	0	1	0	2	None	2 Light	95.40	3617.00
Avg.									80.22	2961.24

Table 4. Sort by % Tripolite

Sample#	Sample Name	Run #	% Chert Slab	% LS Slab	% Trip Slab	Facies	Contact	Frac Amt	RWH Avg	PSI
26	KB 3E	17	0	1	0	1	None	1 None	46.70	1264.20
16	KB 1D	11	0.2	0.8	0	1	Sharp	3 Medium	86.64	4124.80
9	KB 4D	6	0.25	0.75	0	1	Diffuse	4 Heavy	86.65	2202.70
2	KB 4F	2	0.5	0.5	0	1	Sharp	3 Medium	95.05	2939.60
11	KB 2A	8	0.8	0.2	0	1	Sharp	4 Heavy	94.48	3687.50
10	KB 5A	7	0	1	0	2	None	2 Light	95.40	3617.00
24	KB 2G	15	0.4	0.6	0	2	Sharp	3 Medium	86.32	4017.90
7	KB 1B	4	0.5	0.5	0	2	Sharp	4 Heavy	86.65	3088.30
20	KB 1E	12	0.75	0.25	0	2	Sharp	3 Medium	95.20	2013.20
1	KB 2F	1	0.8	0.2	0	2	Diffuse	4 Heavy	91.12	1054.90
5	KB 4B	3	0	1	0	3	None	2 Light	80.30	2007.70
8	KB 1C	5	0.4	0.6	0	3	Sharp	2 Light	85.78	2513.30
29	KB 4A	20	0.7	0.3	0	3	Diffuse	4 Heavy	91.10	778.40
27	KB 2J	18	0.8	0.2	0	3	Diffuse	2 Light	68.48	2942.90
22	KB 2E	14	0.85	0.15	0	3	Diffuse	2 Light	72.50	4251.50
25	KB 2K	16	0.9	0.1	0	3	Diffuse	1 None	75.33	1983.50
30	KB 2I	21	0.95	0.05	0	3	Diffuse	2 Light	86.98	8370.00
34	KB 5F	25	0.97	0.03	0	3	Diffuse	2 Light	89.30	6353.10
13	KB 3A	9	0	1	0	4	None	4 Heavy	82.40	3541.00
35	KB 5G	26	0	0.9	0.1	4	Sharp	2 Light	92.50	2787.60
14	KB 2B	10	0	0.85	0.15	4	Sharp	2 Light	87.66	3058.50
Avg.									84.60	3171.31
33	KB 1F	24	0	0.6	0.4	4	Sharp	1 None	71.60	2302.90
28	KB 5D	19	0	0.55	0.45	4	Sharp	2 Light	60.64	4097.30
Avg.									66.12	3200.10
21	KB 5C	13	0	0.35	0.65	4	Sharp	2 Light	68.74	1445.90
32	KB 2H	23	0	0.35	0.65	4	Sharp	2 Light	61.95	3359.20
31	KB 5E	22	0	0	1	4	None	2 Light	87.80	2888.90
Avg.									72.83	2564.67

Table 5. Sort by Facies

Sample#	Sample Name	Run #	% Chert Slab	% LS Slab	% Trip Slab	Facies	Contact	Frac Amt	RWH Avg	PSI
26	KB 3E	17	0	1	0	1	None	1 None	46.70	1264.20
16	KB 1D	11	0.2	0.8	0	1	Sharp	3 Medium	86.64	4124.80
9	KB 4D	6	0.25	0.75	0	1	Diffuse	4 Heavy	86.65	2202.70
2	KB 4F	2	0.5	0.5	0	1	Sharp	3 Medium	95.05	2939.60
11	KB 2A	8	0.8	0.2	0	1	Sharp	4 Heavy	94.48	3687.50
Avg.									81.90	2843.76
10	KB 5A	7	0.5	0.5	0	2	None	2 Light	95.40	3617.00
24	KB 2G	15	0.4	0.6	0	2	Sharp	3 Medium	86.32	4017.90
7	KB 1B	4	0.5	0.5	0	2	Sharp	4 Heavy	86.65	3088.30
20	KB 1E	12	0.75	0.25	0	2	Sharp	3 Medium	95.20	2013.20
1	KB 2F	1	0.8	0.2	0	2	Diffuse	4 Heavy	91.12	1054.90
Avg.									90.94	2758.26
5	KB 4B	3	0	1	0	3	None	2 Light	80.30	2007.70
14	KB 2B	10	0	0.85	0.15	3	Sharp	2 Light	87.66	3058.50
8	KB 1C	5	0.4	0.6	0	3	Sharp	2 Light	85.78	2513.30
29	KB 4A	20	0.7	0.3	0	3	Diffuse	4 Heavy	91.10	778.40
27	KB 2J	18	0.8	0.2	0	3	Diffuse	2 Light	85.60	2942.90
22	KB 2E	14	0.85	0.15	0	3	Diffuse	2 Light	72.50	4251.50
25	KB 2K	16	0.9	0.1	0	3	Diffuse	1 None	83.70	1983.50
30	KB 2I	21	0.95	0.05	0	3	Diffuse	2 Light	86.98	8370.00
34	KB 5F	25	0.97	0.03	0	3	Diffuse	2 Light	89.30	6353.10
Avg.									84.20	3584.32
13	KB 3A	9	0	1	0	4	None	4 Heavy	82.40	3541.00
21	KB 5C	13	0	0.35	0.65	4	Sharp	1 Light	68.74	1445.90
28	KB 5D	19	0	0.55	0.45	4	Sharp	2 Light	60.64	4097.30
31	KB 5E	22	0	0	100	4	None	2 Light	87.80	2888.90
32	KB 2H	23	0	0.35	0.65	4	Sharp	2 Light	61.95	3359.20
33	KB 1F	24	0	0.6	0.4	4	Sharp	1 None	71.60	2302.90
35	KB 5G	26	0	0.1	0.9	4	Sharp	2 Light	92.50	2787.60
Avg.									72.83	2917.54

Table 6. Sort by Fracture Amount

Sample#	Sample Name		% Chert Slab	% LS Slab	% Trip Slab	Facies	Contact	Frac Amt	RWH Avg	PSI
26	KB	3E	0	1	0	1	None	1 None	46.70	1264.20
25	KB	2K	0.9	0.1	0	3	Diffuse	1 None	83.70	1983.50
33	KB	1F	0	0.6	0.4	4	Sharp	1 None	71.60	2302.90
Avg.									67.33	1850.20
21	KB	5C	0	0.35	0.65	4	Sharp	2 Light	68.74	1445.90
10	KB	5A	0.5	0.5	0	2	None	2 Light	95.40	3617.00
5	KB	4B	0	1	0	3	None	2 Light	80.30	2007.70
14	KB	2B	0	0.85	0.15	4	Sharp	2 Light	87.66	3058.50
8	KB	1C	0.4	0.6	0	3	Sharp	2 Light	85.78	2513.30
27	KB	2J	0.8	0.2	0	3	Diffuse	2 Light	85.60	2942.90
22	KB	2E	0.85	0.15	0	3	Diffuse	2 Light	72.50	4251.50
30	KB	2I	0.95	0.05	0	3	Diffuse	2 Light	86.98	8370.00
34	KB	5F	0.97	0.03	0	3	Diffuse	2 Light	89..3	6353.10
28	KB	5D	0	0.55	0.45	4	Sharp	2 Light	60.64	4097.30
31	KB	5E	0	0	100	4	None	2 Light	87.80	2888.90
32	KB	2H	0	0.35	0.65	4	Sharp	2 Light	61.95	3359.20
0.1	KB	5G	0	0.1	0.9	4	Sharp	2 Light	92.50	2787.60
Avg.									80.49	3668.68
16	KB	1D	0.2	0.8	0	1	Sharp	3 Medium	86.64	4124.80
2	KB	4F	0.5	0.5	0	1	Sharp	3 Medium	95.05	2939.60
24	KB	2G	0.4	0.6	0	2	Sharp	3 Medium	86.32	4017.90
20	KB	1E	0.75	0.25	0	2	Sharp	3 Medium	95.20	2013.20
Avg.									90.80	3273.88
9	KB	4D	0.25	0.75	0	1	Diffuse	4 Heavy	86.65	2202.70
11	KB	2A	0.8	0.2	0	1	Sharp	4 Heavy	94.48	3687.50
7	KB	1B	0.5	0.5	0	2	Sharp	4 Heavy	86.65	3088.30
1	KB	2F	0.8	0.2	0	2	Diffuse	4 Heavy	91.12	1054.90
29	KB	4A	0.7	0.3	0	3	Diffuse	4 Heavy	91.10	778.40
13	KB	3A	0	1	0	4	None	4 Heavy	82.40	3541.00
Avg.									88.73	2392.13

Table 7. Sort by Contact Type

Sample#	Sample	Name	Run #	% Chert Slab	% LS Slab	% Trip Slab	Facies	Contact	Frac Amt	RWH Avg	PSI
9	KB	4D	6	0.25	0.75	0	1	Diffuse	4 Heavy	86.65	2202.70
1	KB	2F	1	0.8	0.2	0	2	Diffuse	4 Heavy	91.12	1054.90
29	KB	4A	20	0.7	0.3	0	3	Diffuse	4 Heavy	91.10	778.40
27	KB	2J	18	0.8	0.2	0	3	Diffuse	2 Light	85.60	2942.90
22	KB	2E	14	0.85	0.15	0	3	Diffuse	2 Light	72.50	4251.50
25	KB	2K	16	0.9	0.1	0	3	Diffuse	1 None	83.70	1983.50
30	KB	2I	21	0.95	0.05	0	3	Diffuse	2 Light	86.98	8370.00
34	KB	5F	25	0.97	0.03	0	3	Diffuse	2 Light	89.30	6353.10
Avg.										85.87	3492.13
26	KB	3E	17	0	1	0	1	None	1 None	46.70	1264.20
10	KB	5A	7	0.5	0.5	0	2	None	2 Light	95.40	3617.00
5	KB	4B	3	0	1	0	3	None	2 Light	80.30	2007.70
13	KB	3A	9	0	1	0	4	None	4 Heavy	82.40	3541.00
31	KB	5E	22	0	0	100	4	None	2 Light	87.80	2888.90
Avg.										78.52	2663.76
16	KB	1D	11	0.2	0.8	0	1	Sharp	3 Medium	86.64	4124.80
2	KB	4F	2	0.5	0.5	0	1	Sharp	3 Medium	95.05	2939.60
11	KB	2A	8	0.8	0.2	0	1	Sharp	4 Heavy	94.48	3687.50
24	KB	2G	15	0.4	0.6	0	2	Sharp	3 Medium	86.32	4017.90
7	KB	1B	4	0.5	0.5	0	2	Sharp	4 Heavy	86.65	3088.30
20	KB	1E	12	0.75	0.25	0	2	Sharp	3 Medium	95.20	2013.20
14	KB	2B	10	0	0.85	0.15	4	Sharp	2 Light	87.66	3058.50
8	KB	1C	5	0.4	0.6	0	3	Sharp	2 Light	85.78	2513.30
21	KB	5C	13	0	0.35	0.65	4	Sharp	1 Light	68.74	1445.90
28	KB	5D	19	0	0.55	0.45	4	Sharp	2 Light	60.64	4097.30
32	KB	2H	23	0	0.35	0.65	4	Sharp	2 Light	61.95	3359.20
33	KB	1F	24	0	0.6	0.4	4	Sharp	1 None	71.60	2302.90
35	KB	5G	26	0	0.1	0.9	4	Sharp	2 Light	92.50	2787.60
Avg.										82.55	3033.54

Table 8. Sort by Rockwell Hardness

Sample#	Sample	Name	Run #	% Chert Slab	% LS Slab	% Trip Slab	Facies	Contact	Frac Amt	RWH Avg	PSI
26	KB	3E	17	0	1	0	1	None	1 None	46.70	1264.20
28	KB	5D	19	0	0.55	0.45	4	Sharp	2 Light	60.64	4097.30
32	KB	2H	23	0	0.35	0.65	4	Sharp	2 Light	61.95	3359.20
21	KB	5C	13	0	0.35	0.65	4	Sharp	2 Light	68.74	1445.90
33	KB	1F	24	0	0.6	0.4	4	Sharp	1 None	71.60	2302.90
22	KB	2E	14	0.85	0.15	0	3	Diffuse	2 Light	72.50	4251.50
5	KB	4B	3	0	1	0	3	None	2 Light	80.30	2007.70
13	KB	3A	9	0	1	0	4	None	4 Heavy	82.40	3541.00
25	KB	2K	16	0.9	0.1	0	3	Diffuse	1 None	83.70	1983.50
27	KB	2J	18	0.8	0.2	0	3	Diffuse	2 Light	85.60	2942.90
8	KB	1C	5	0.4	0.6	0	3	Sharp	2 Light	85.78	2513.30
24	KB	2G	15	0.4	0.6	0	2	Sharp	3 Medium	86.32	4017.90
16	KB	1D	11	0.2	0.8	0	1	Sharp	3 Medium	86.64	4124.80
7	KB	1B	4	0.5	0.5	0	2	Sharp	4 Heavy	86.65	3088.30
9	KB	4D	6	0.25	0.75	0	1	Diffuse	4 Heavy	86.65	2202.70
30	KB	2I	21	0.95	0.05	0	3	Diffuse	2 Light	86.98	8370.00
14	KB	2B	10	0	0.85	0.15	4	Sharp	2 Light	87.66	3058.50
31	KB	5E	22	0	0	100	4	None	2 Light	87.80	2888.90
34	KB	5F	25	0.97	0.03	0	3	Diffuse	2 Light	89.30	6353.10
29	KB	4A	20	0.7	0.3	0	3	Diffuse	4 Heavy	91.10	778.40
1	KB	2F	1	0.8	0.2	0	2	Diffuse	4 Heavy	91.12	1054.90
35	KB	5G	26	0	0.1	0.9	4	Sharp	2 Light	92.50	2787.60
11	KB	2A	8	0.8	0.2	0	1	Sharp	4 Heavy	94.48	3687.50
2	KB	4F	2	0.5	0.5	0	1	Sharp	3 Medium	95.05	2939.60
20	KB	1E	12	0.75	0.25	0	2	Sharp	3 Medium	95.20	2013.20
10	KB	5A	7	0.5	0.5	0	2	None	2 Light	95.40	3617.00

Table 9. Sort by Compressive Strength

Sample#	Sample Name	Run #	% Chert Slab	% LS Slab	% Trip Slab	Facies	Contact	Frac Amt	RWH Avg	PSI
29	KB 4A	20	0.70	0.30	0.00	3	Diffuse	4 Heavy	91.10	778.40
1	KB 2F	1	0.80	0.20	0.00	2	Diffuse	4 Heavy	91.12	1054.90
26	KB 3E	17	0.00	1.00	0.00	1	None	1 None	46.70	1264.20
21	KB 5C	13	0.00	0.35	0.65	4	Sharp	2 Light	68.74	1445.90
25	KB 2K	16	0.90	0.10	0.00	3	Diffuse	1 None	83.70	1983.50
5	KB 4B	3	0.00	1.00	0.00	3	None	2 Light	80.30	2007.70
20	KB 1E	12	0.75	0.25	0.00	2	Sharp	3 Medium	95.20	2013.20
9	KB 4D	6	0.25	0.75	0.00	1	Diffuse	4 Heavy	86.65	2202.70
33	KB 1F	24	0.00	0.60	0.40	4	Sharp	1 None	71.60	2302.90
8	KB 1C	5	0.40	0.60	0.00	3	Sharp	2 Light	85.78	2513.30
35	KB 5G	26	0.00	0.90	0.10	4	Sharp	2 Light	92.50	2787.60
31	KB 5E	22	0.00	0.00	1.00	4	None	2 Light	87.80	2888.90
2	KB 4F	2	0.50	0.50	0.00	1	Sharp	3 Medium	95.05	2939.60
27	KB 2J	18	0.80	0.20	0.00	3	Diffuse	2 Light	85.60	2942.90
14	KB 2B	10	0.00	0.85	0.15	4	Sharp	2 Light	87.66	3058.50
7	KB 1B	4	0.50	0.50	0.00	2	Sharp	4 Heavy	86.65	3088.30
32	KB 2H	23	0.00	0.35	0.65	4	Sharp	2 Light	61.95	3359.20
13	KB 3A	9	0.00	1.00	0.00	4	None	4 Heavy	82.40	3541.00
10	KB 5A	7	0.00	1.00	0.00	2	None	2 Light	95.40	3617.00
11	KB 2A	8	0.80	0.20	0.00	1	Sharp	4 Heavy	94.48	3687.50
24	KB 2G	15	0.40	0.60	0.00	2	Sharp	3 Medium	86.32	4017.90
28	KB 5D	19	0.00	0.55	0.45	4	Sharp	2 Light	60.64	4097.30
16	KB 1D	11	0.20	0.80	0.00	1	Sharp	3 Medium	86.64	4124.80
22	KB 2E	14	0.85	0.15	0.00	3	Diffuse	2 Light	72.50	4251.50
34	KB 5F	25	0.97	0.03	0.00	3	Diffuse	2 Light	89.30	6353.10
30	KB 2I	21	0.95	0.05	0.00	3	Diffuse	2 Light	86.98	8370.00

XI. FIGURES

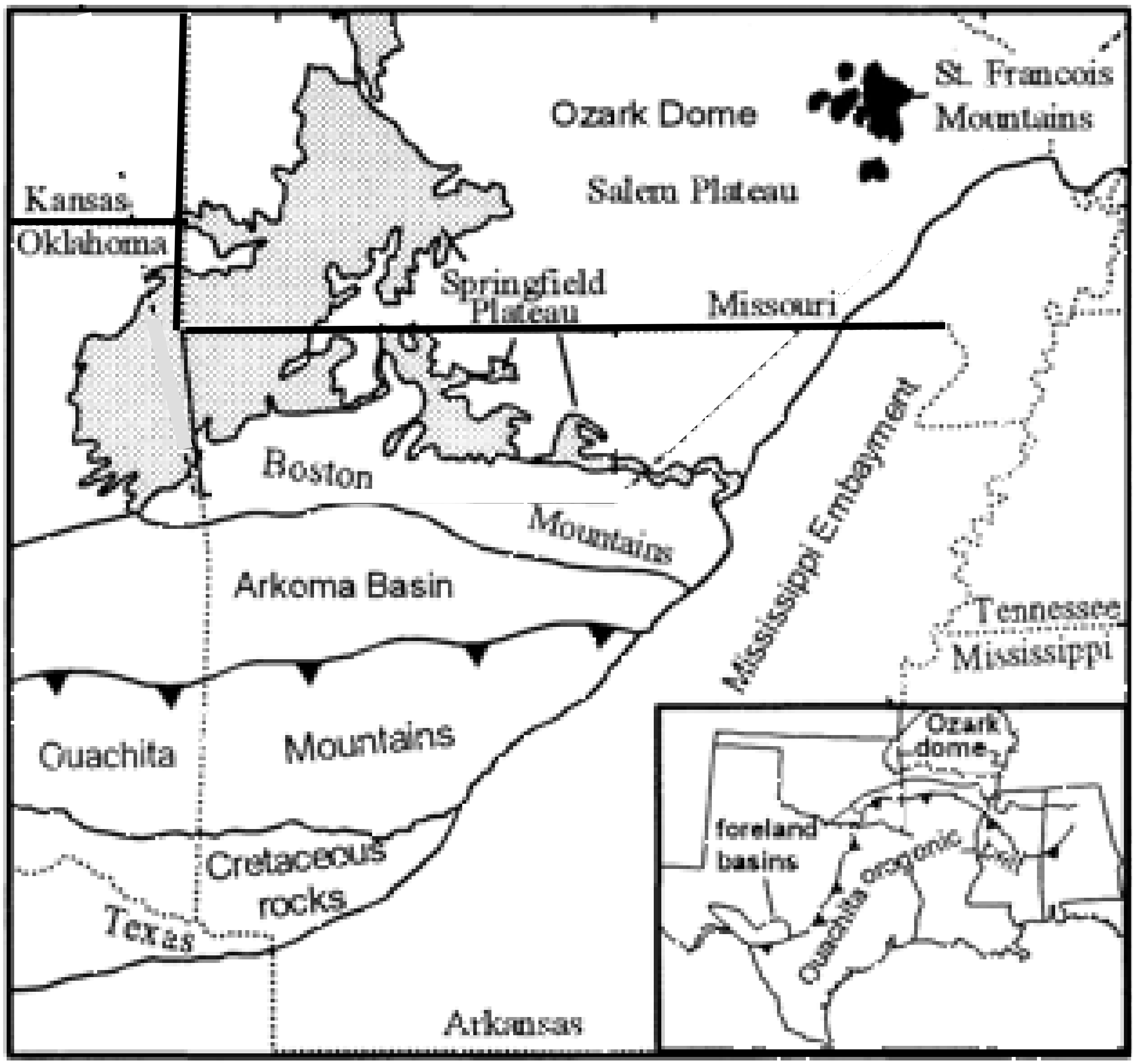

Figure 1. Ozark Dome, Springfield Plateau. Hudson, 2000

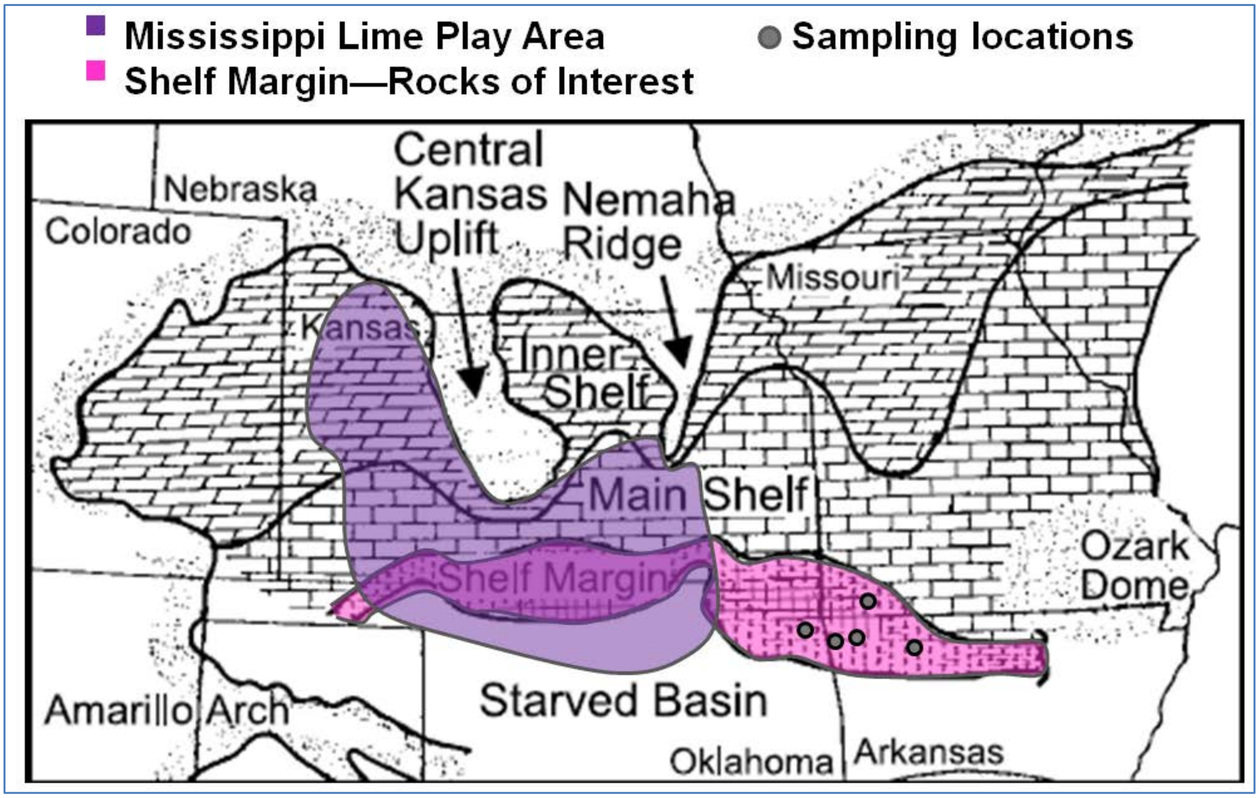

Figure 2. Modified from Watney et al., 2001. Shows area of reservoir, the divisions of the Mississippian carbonate shelf at the time of deposition, and the sampling locations for this thesis.

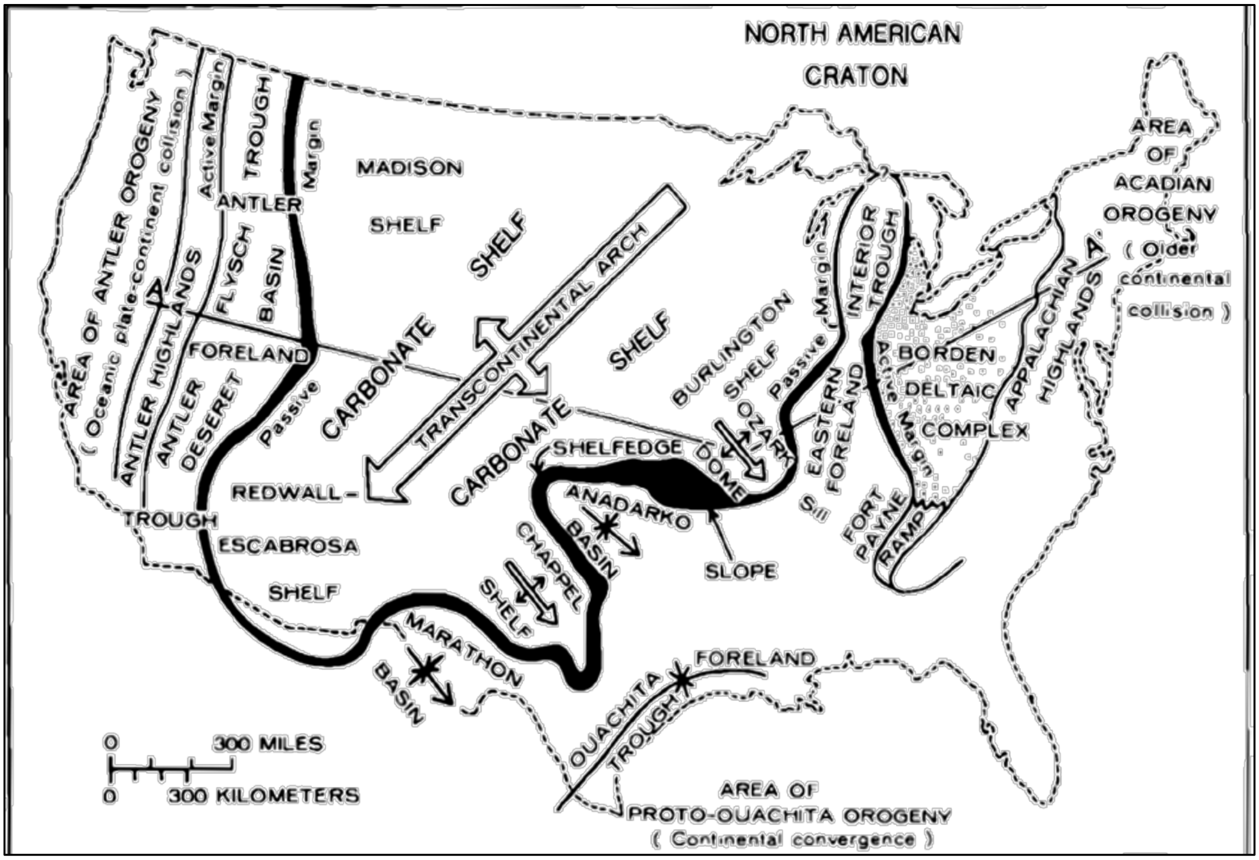

Figure 3. Gutshick and Sandberg (1983). Mississippian paleomap of the current United States.

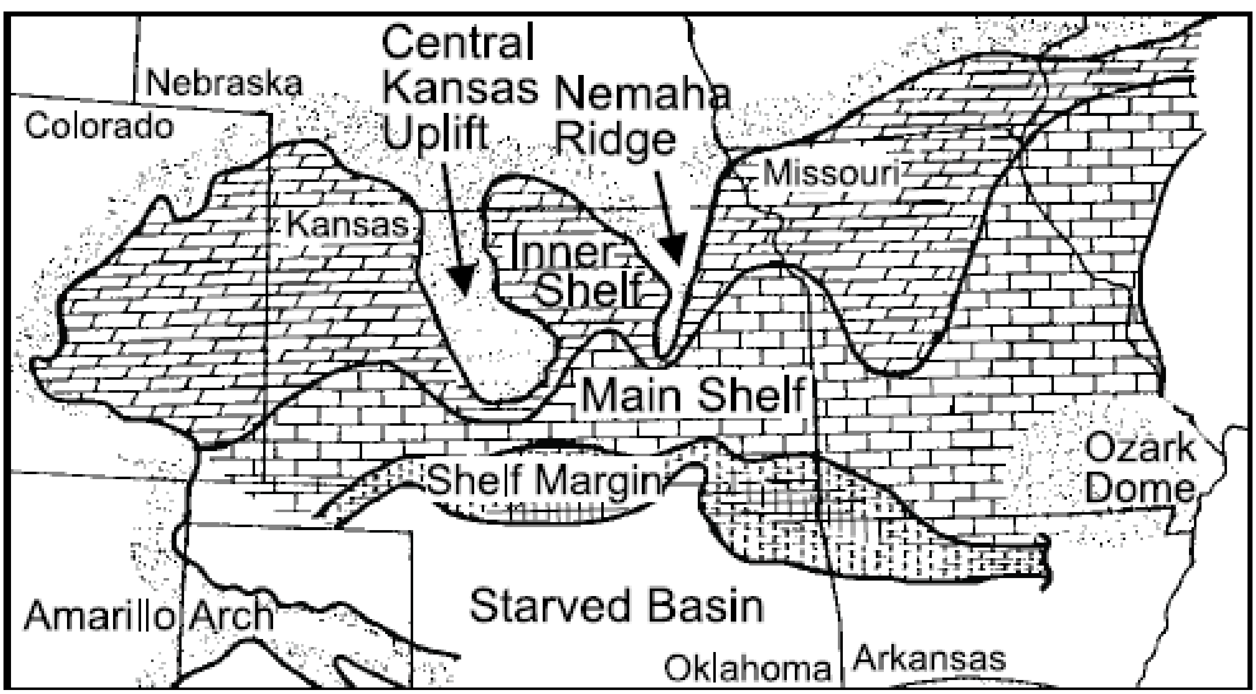

Figure 4. Watney et. al 2001. Mississippian shelf divisions on current state map.

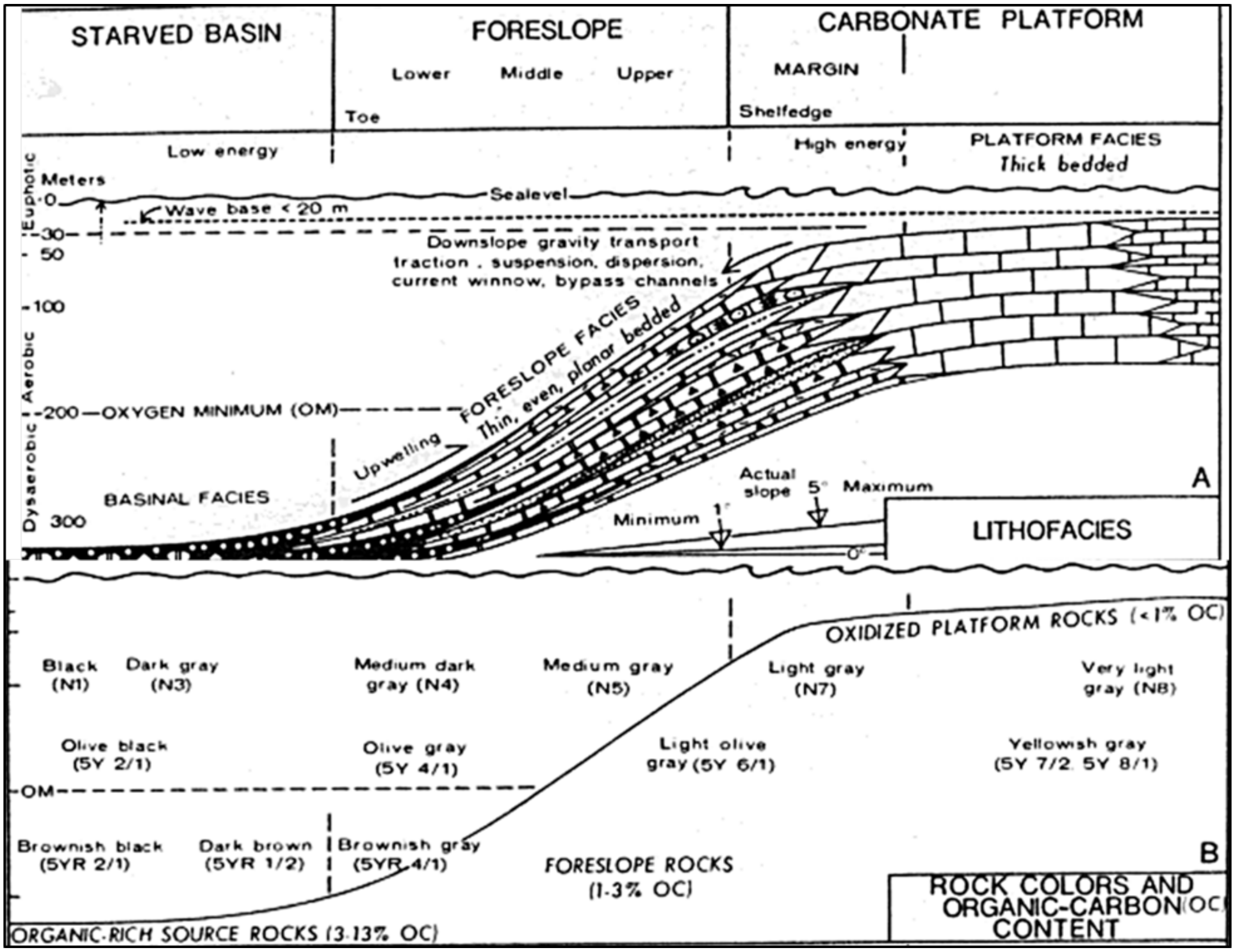

Figure 5. Gutshick and Sandberg (1983)

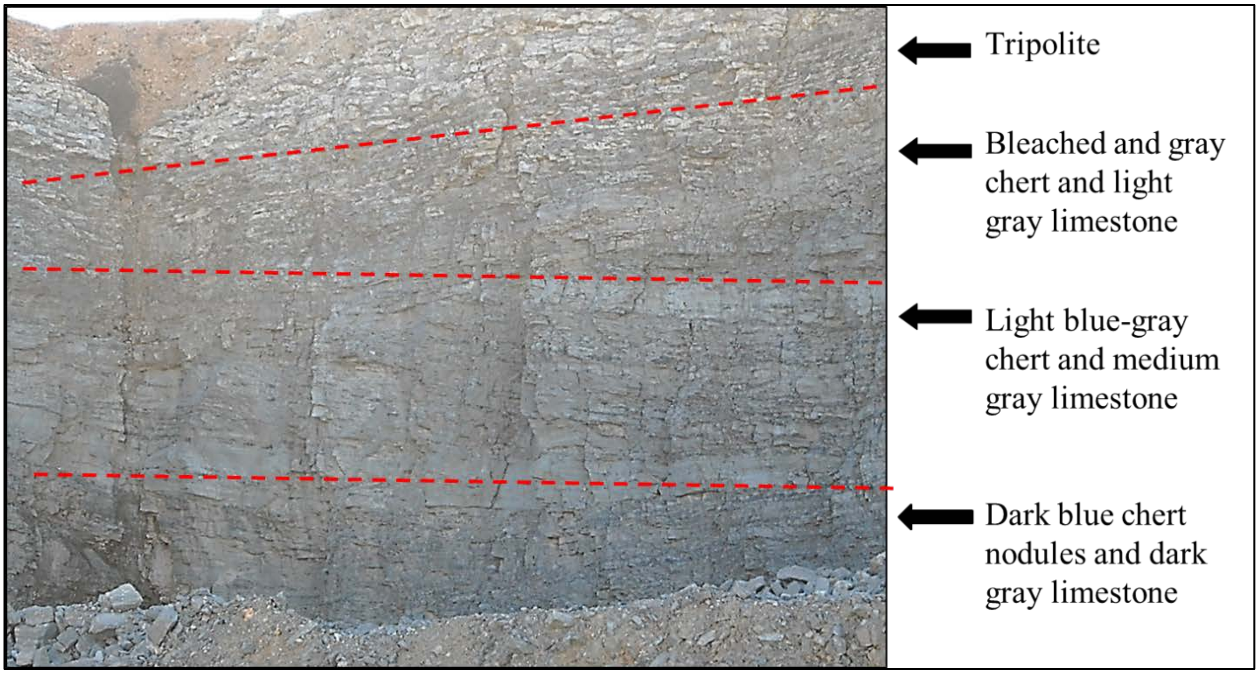

Figure 6. Hindsville Quarry, Arkansas. Photo by Daniel Smith

Figure 7. Hindsville Quarry, Arkansas. Photo by Daniel Smith

Figure 8. Jane, Missouri. Photo by Karen Buckland

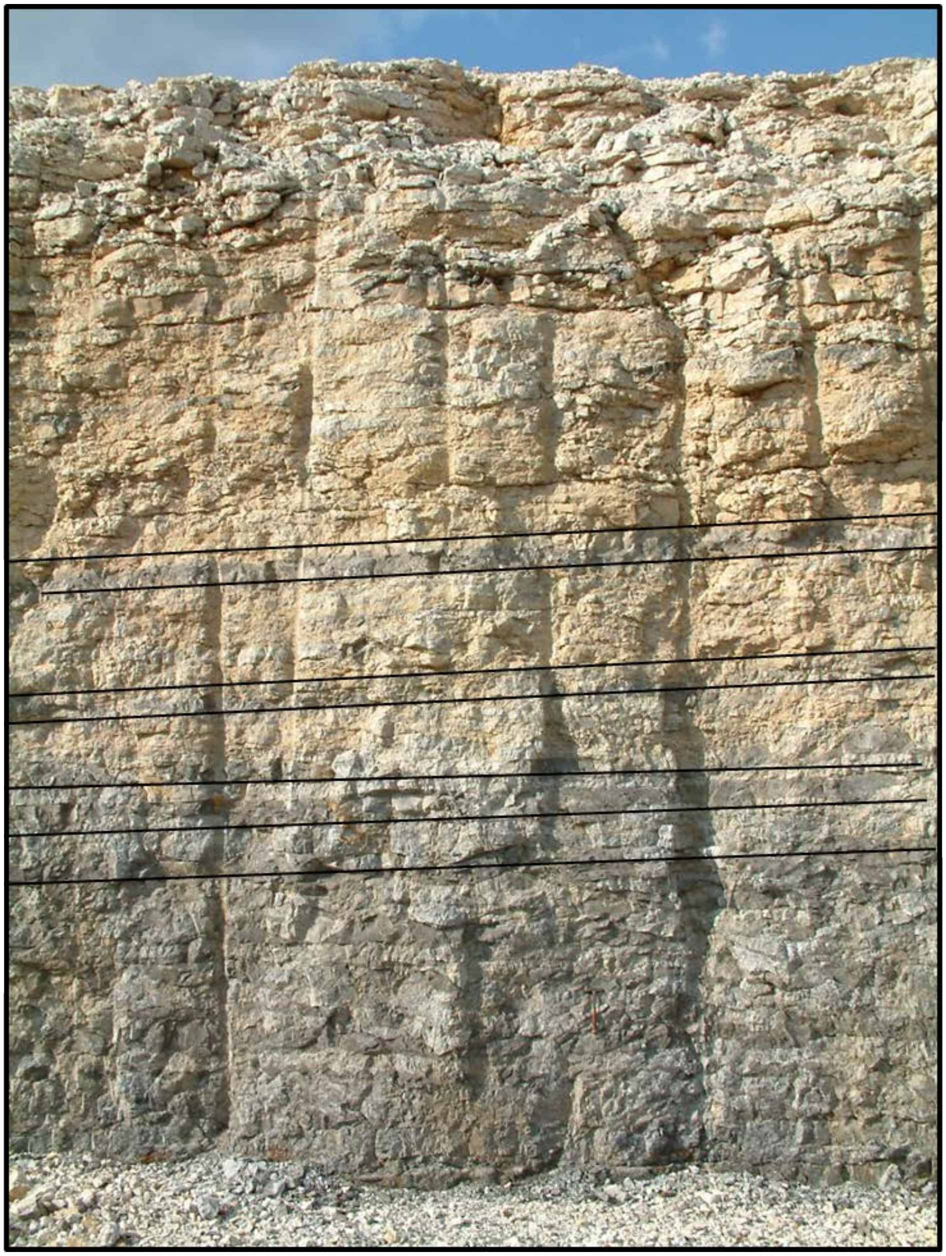

Figure 9. Jane, MO, Highway 71. Photo by Karen Buckland

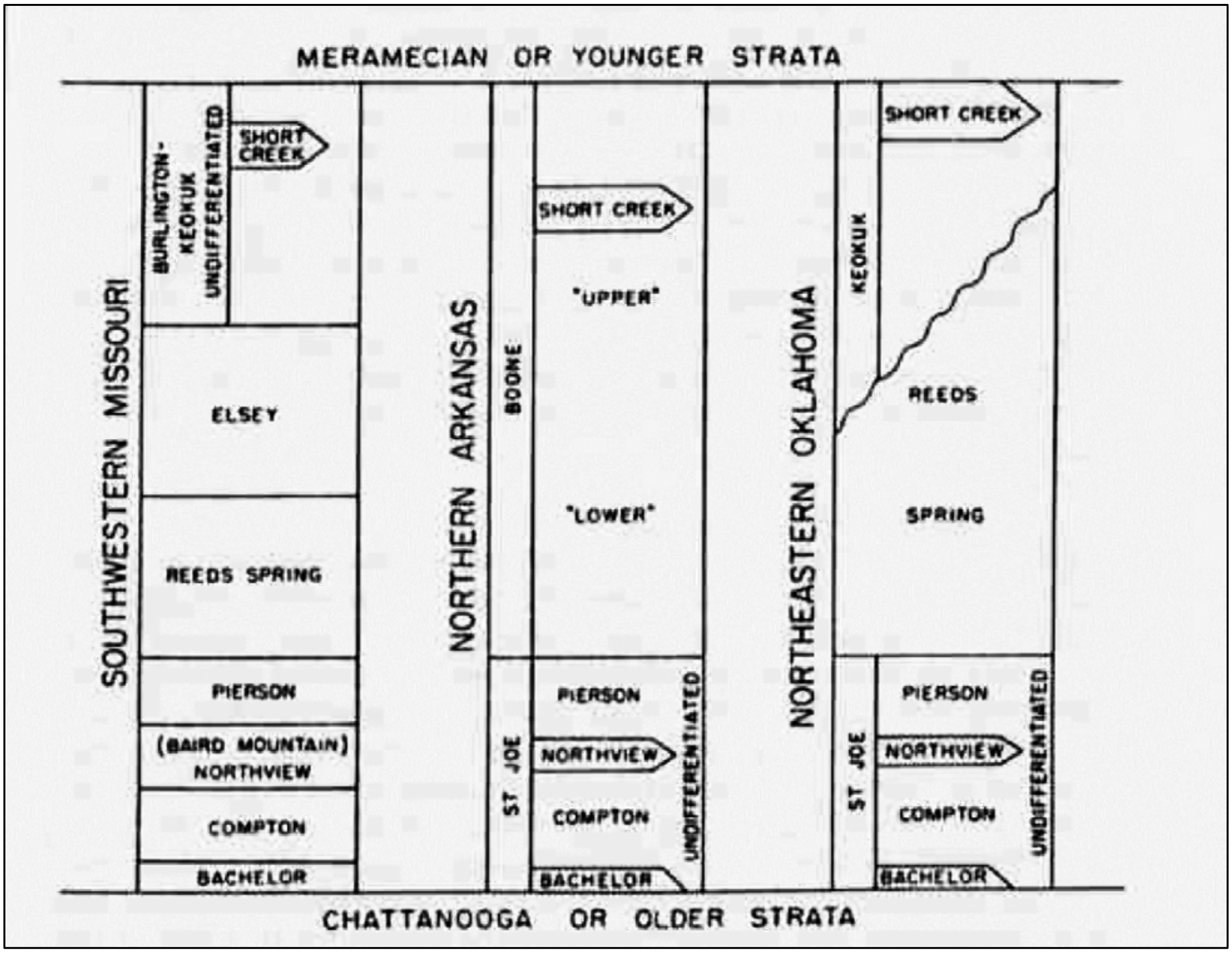

Figure 10. Shelby (1986). Stratigraphic column showing nomenclature by state for Mississippian limestone.

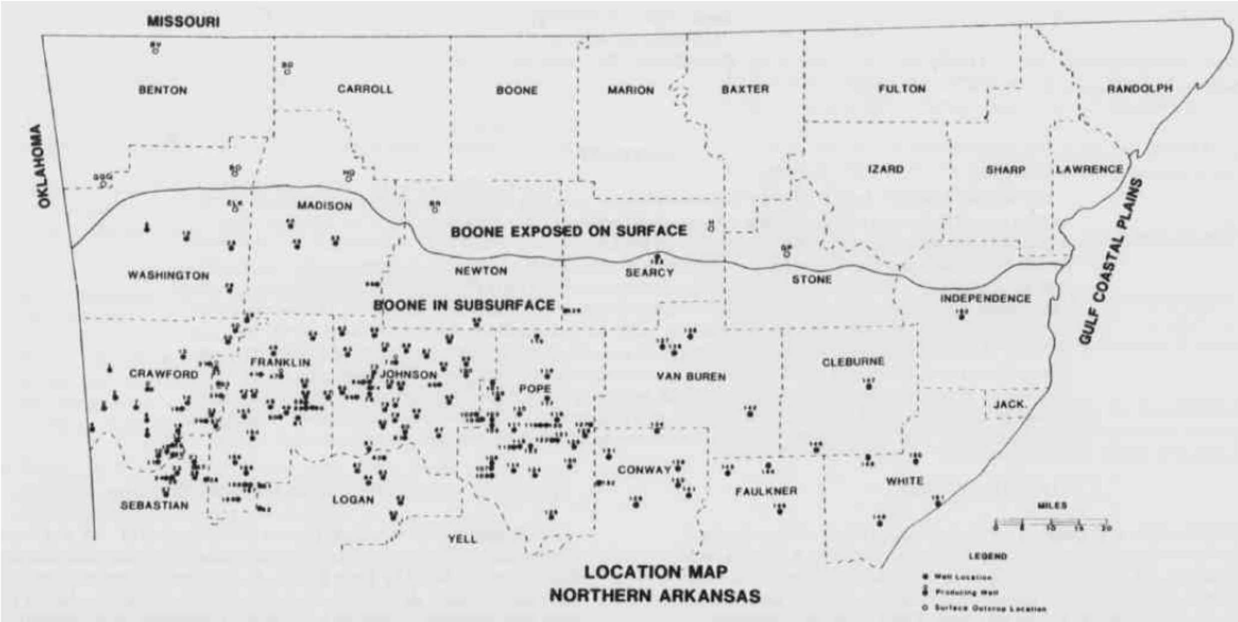

Figure 11. Shelby, 1986. Extent of the Boone Formation in northern Arkansas.

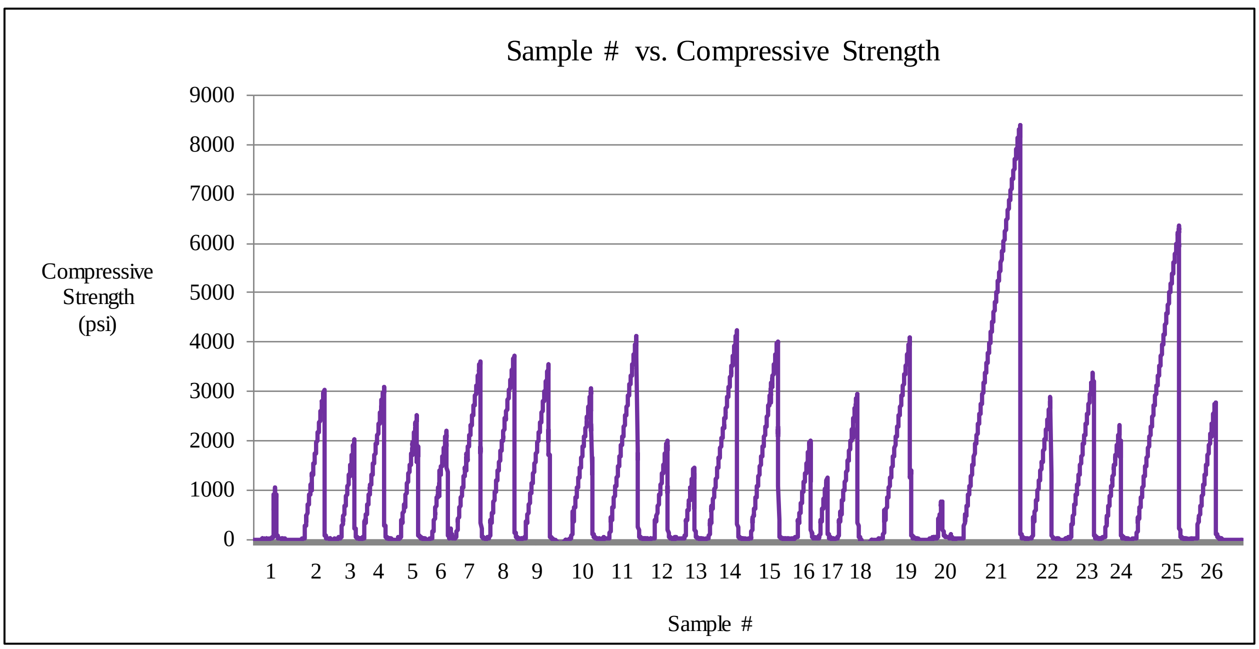

Figure 12. This strength plot shows the range of brittle compressive strength for the 26 samples.

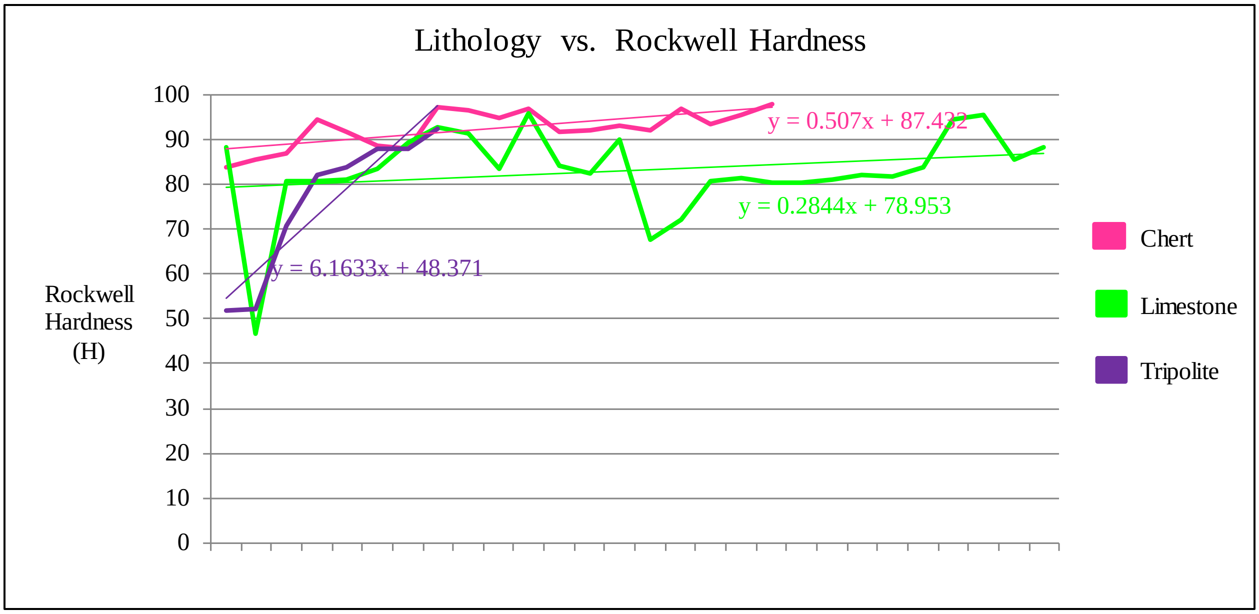

Figure 13. The chert trend is the strongest of the three types of lithology. The limestone clearly is weaker than the chert. The tripolite does not produce a trend that is comparable to the chert and limestone. The tripolite Rockwell Hardness has a steep slope that crosses both the limestone and chert trend lines.

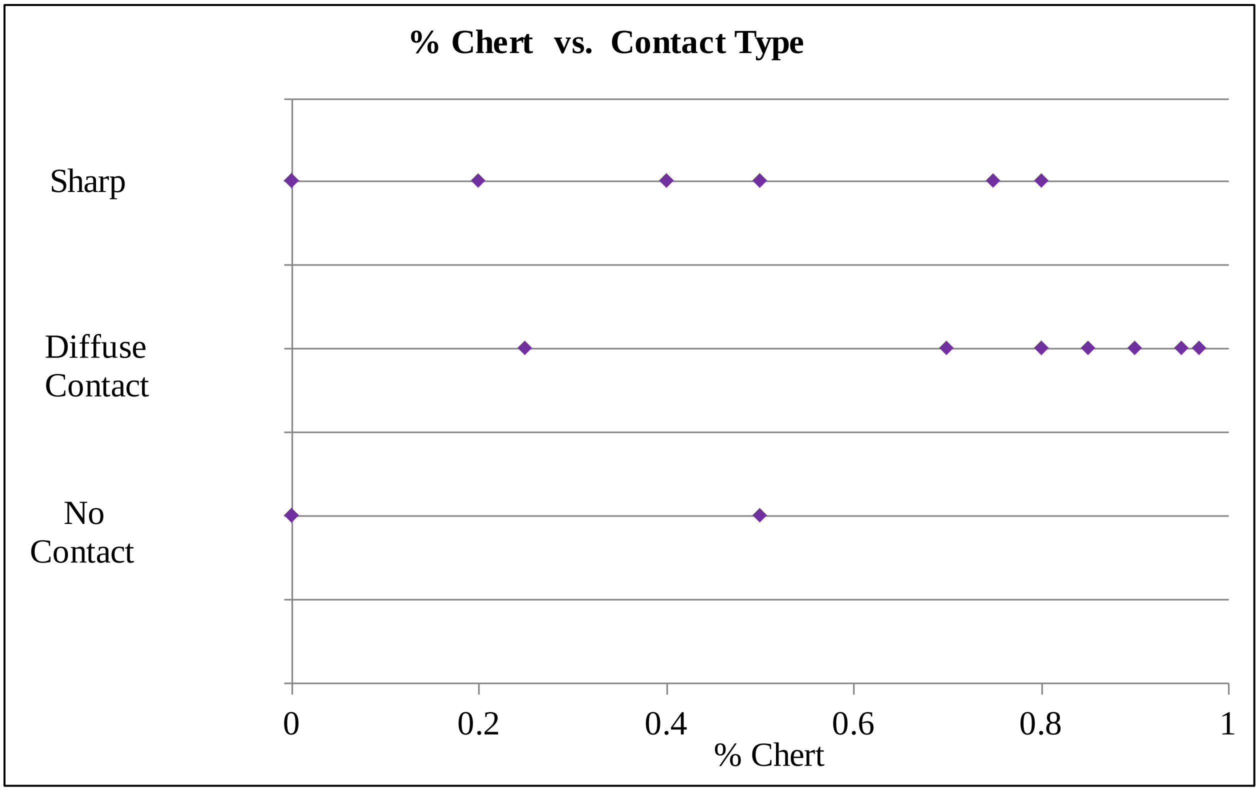

Figure 14. Samples with less than 50% chert lithology favor sharp contact zones or no contact zones. Samples with greater than 70% chert lithology favor diffuse contact zones.

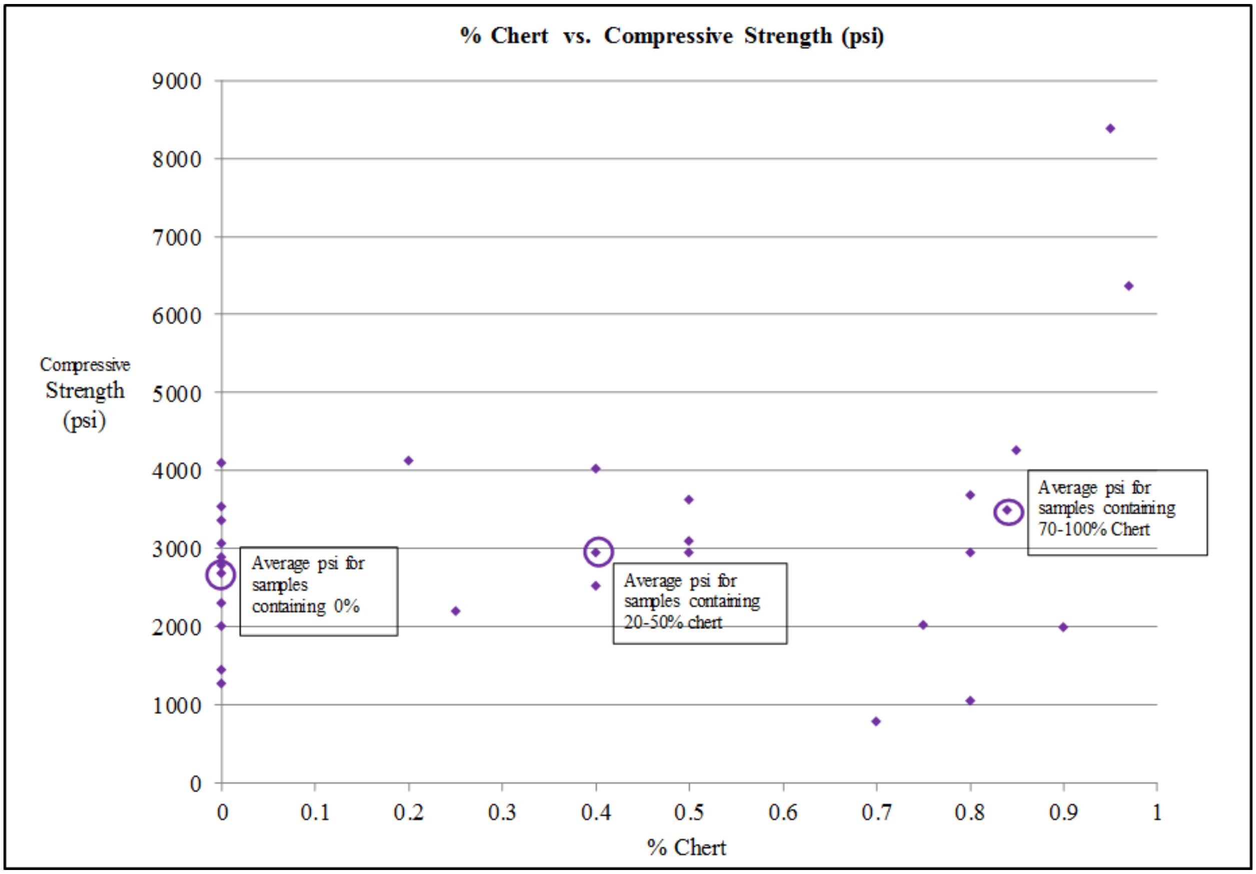

Figure 15. Compressive strength increases as the percent of chert in the sample increases.

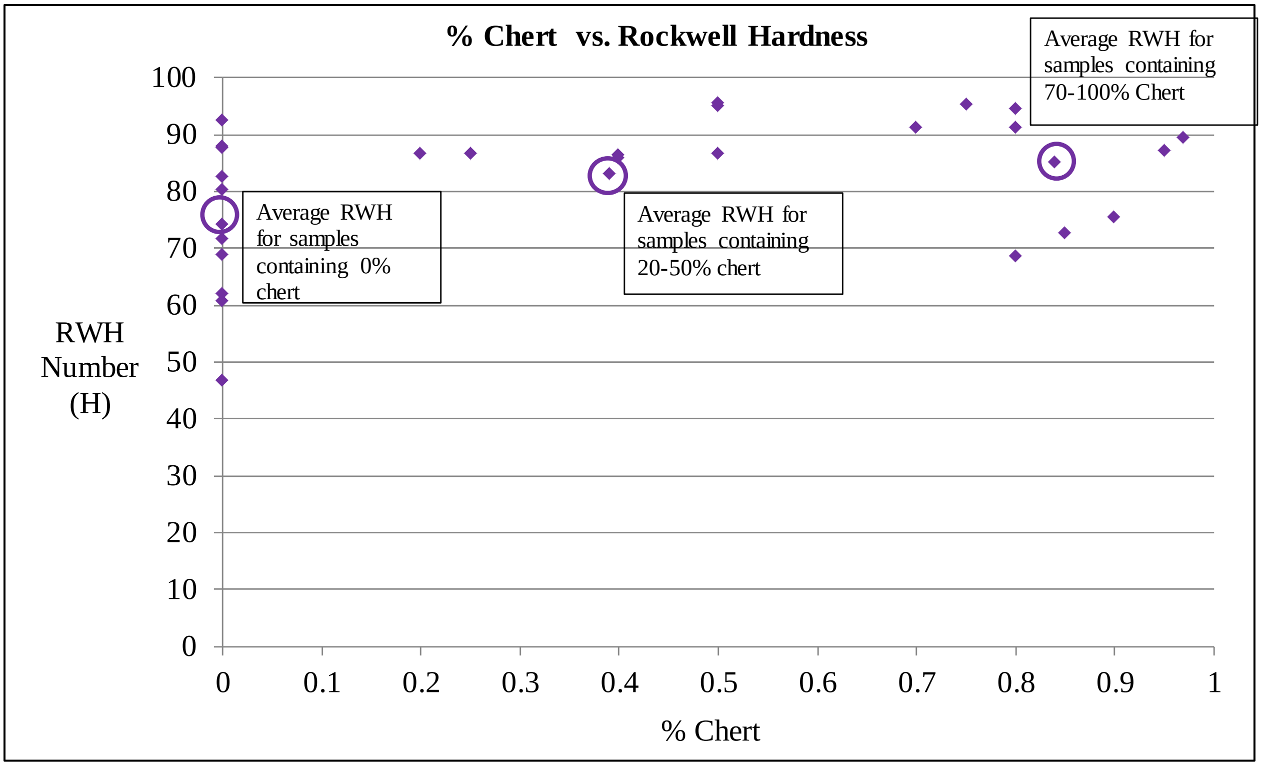

Figure 16. Rockwell Hardness value increases as the percent of chert in the sample increases.

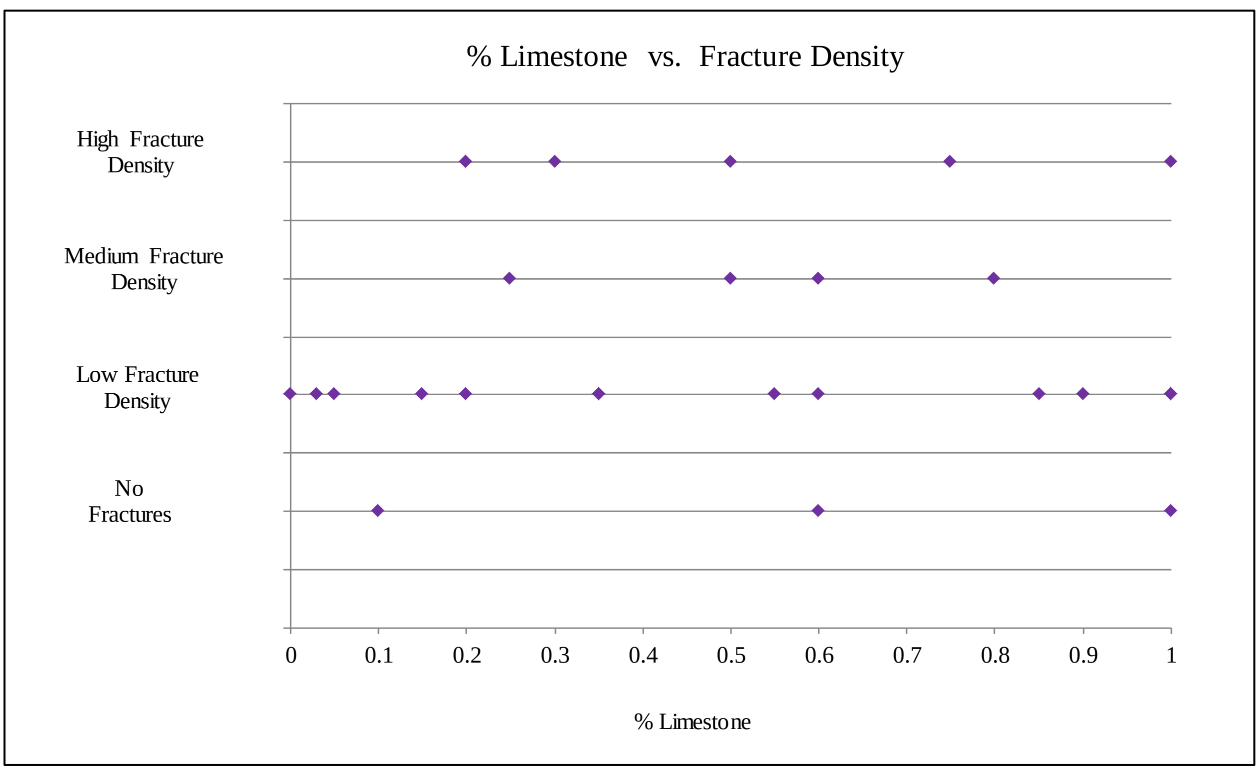

Figure 17. Samples with less than 20% limestone lithology favor low fracture density.

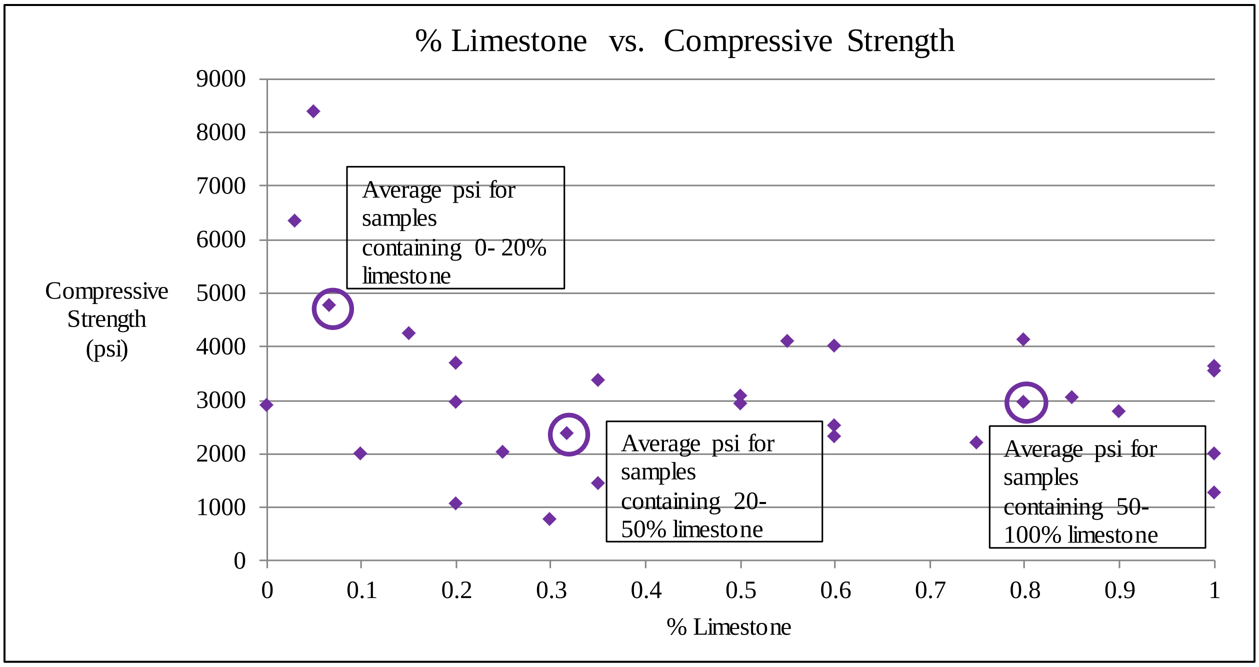

Figure 18. Samples with less than 20% limestone lithology have the highest average compressive strength.

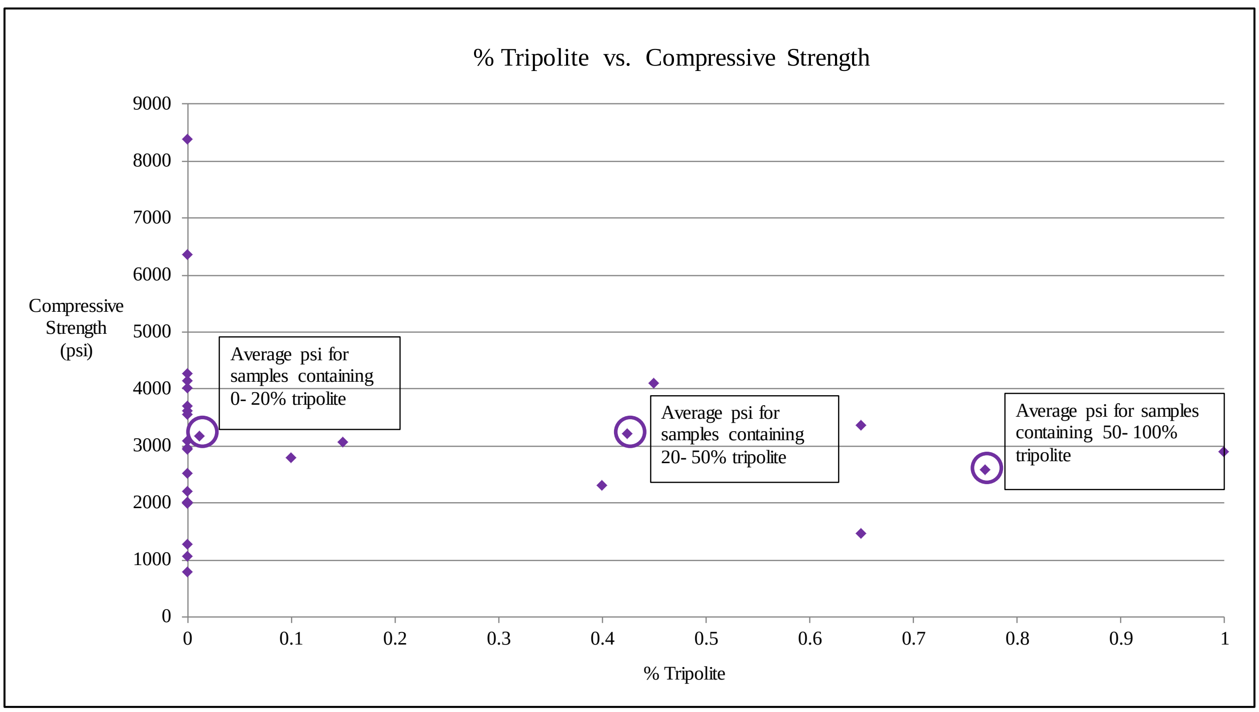

Figure 19. Samples containing greater than 70% tripolite have the lowest average compressive strength.

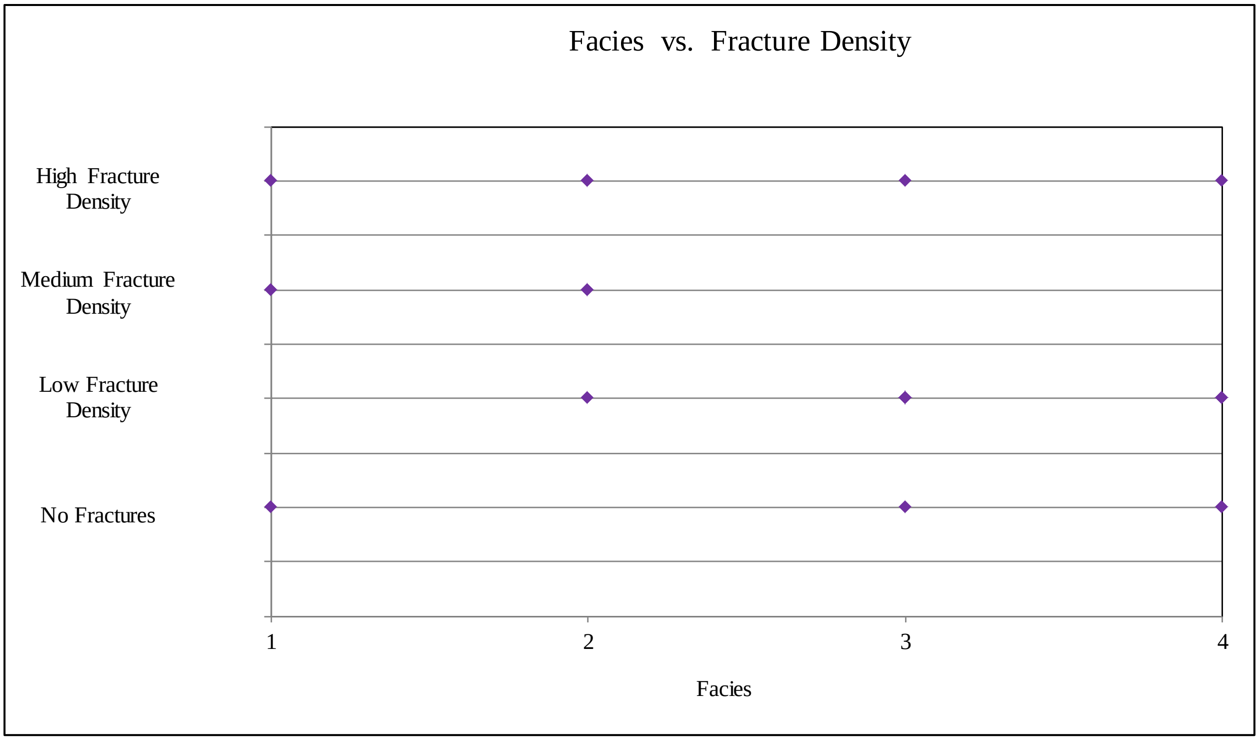

Figure 20. Samples from Facies 1 and 2 tend to have higher fracture density than samples from Facies 3 and 4.

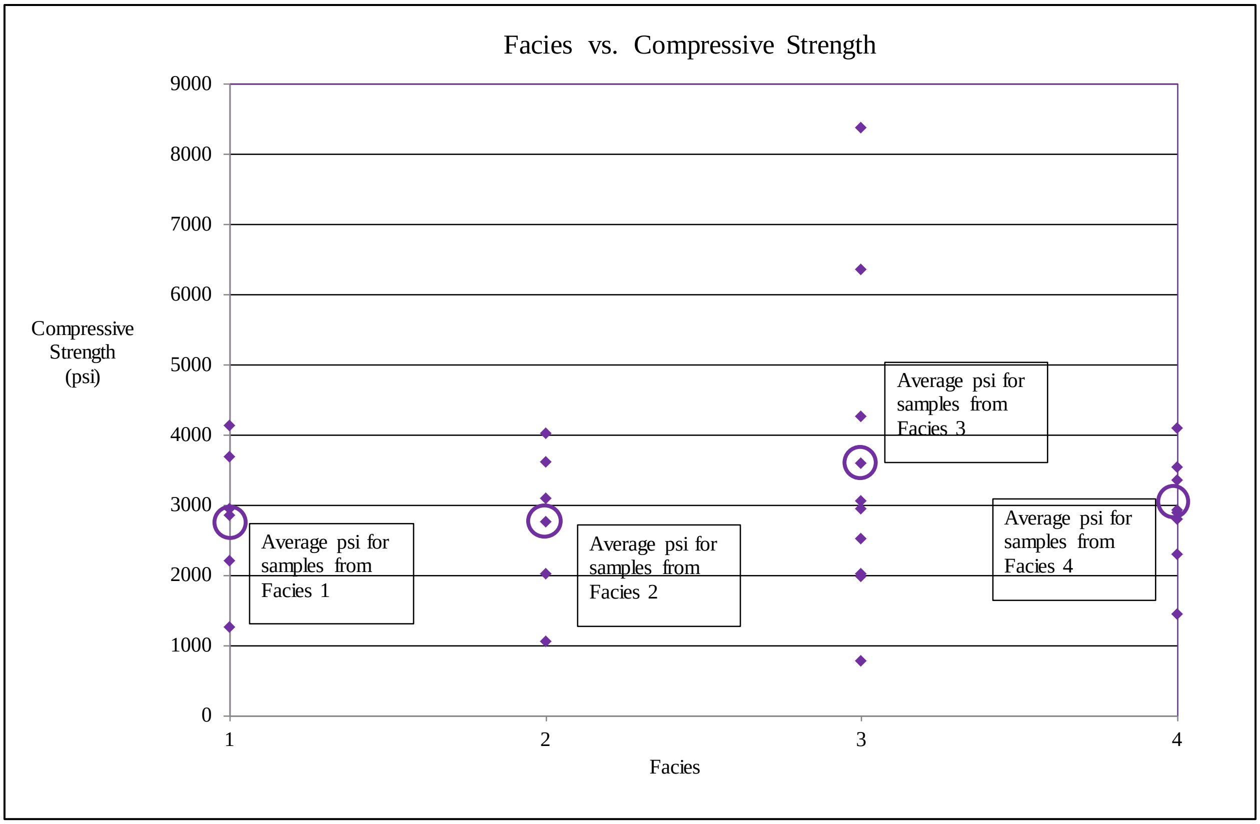

Figure 21. Facies 3 (bleached chert) has the highest average compressive strength. The other three facies types are relatively close in average compressive strength.

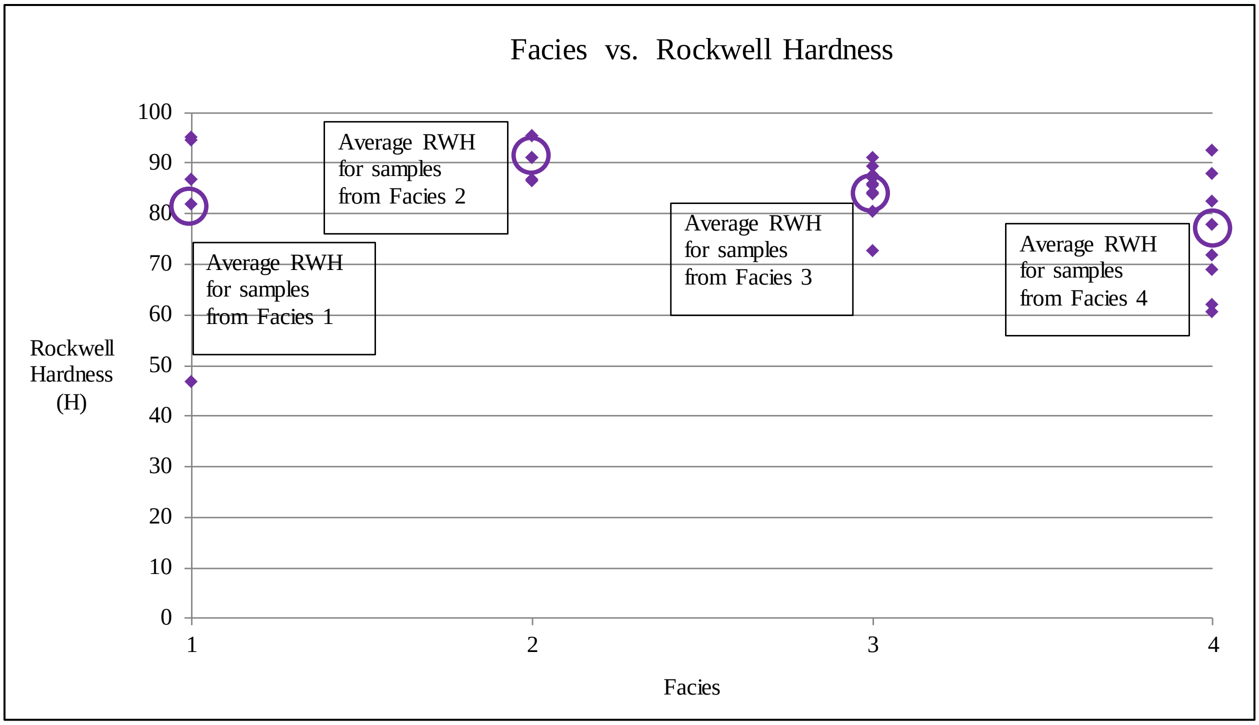

Figure 22. Facies 4 (tripolite) has the lowest average Rockwell Hardness value and Facies 2 (medium blue-gray chert) has the highest average Rockwell Hardness value.

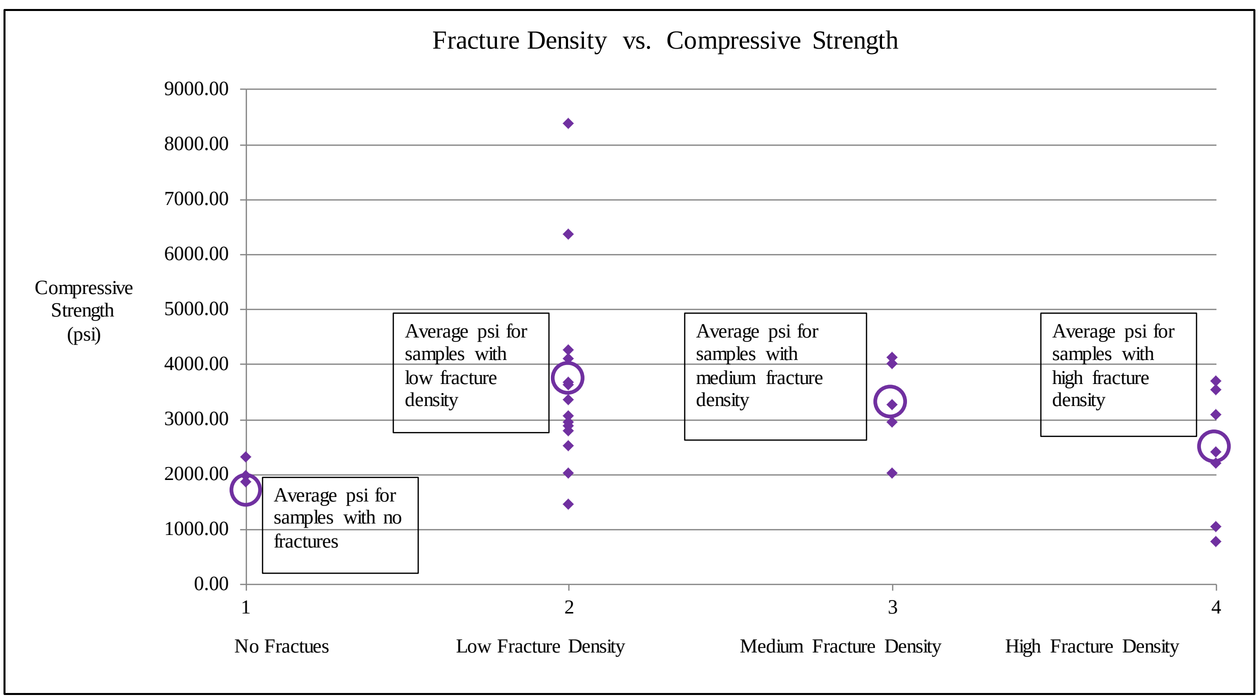

Figure 23. Samples with low fracture density have the highest compress strength.

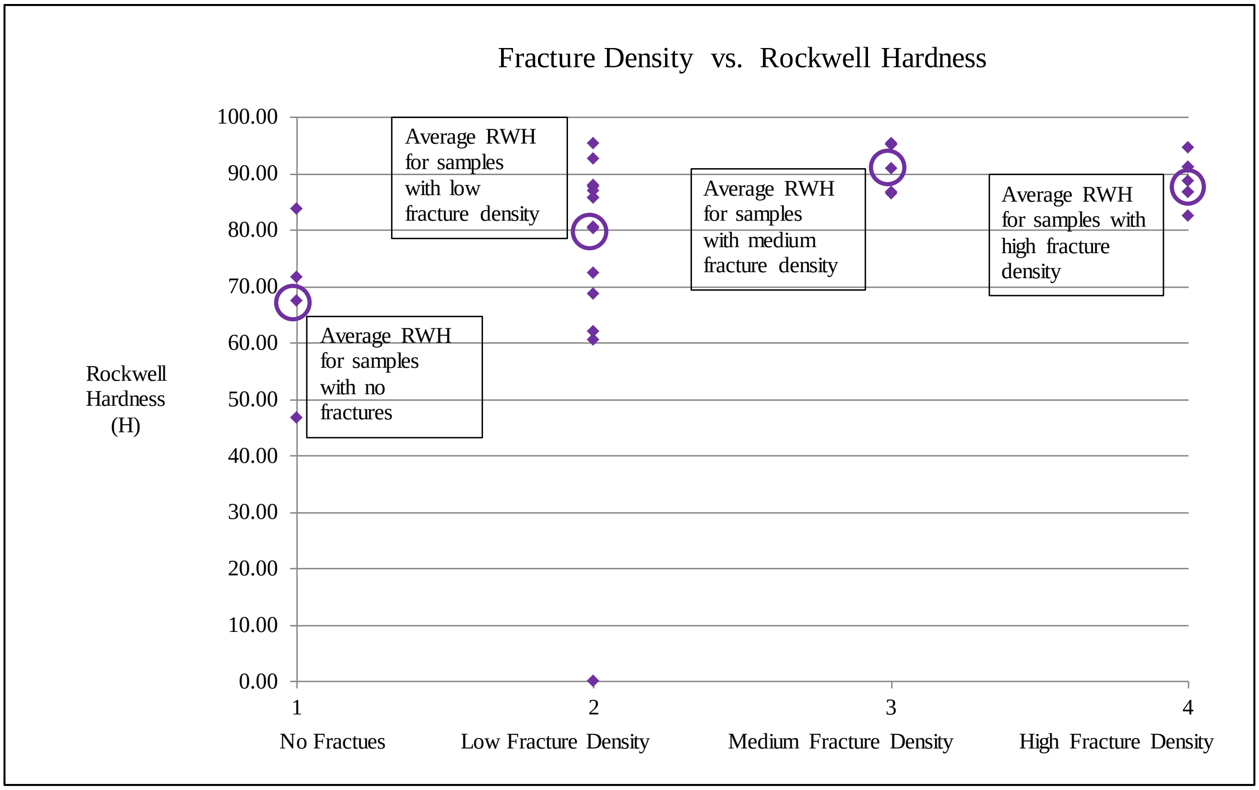

Figure 24. The samples with medium fracture density have the highest average Rockwell Hardness values. The samples without fractures have the lowest average Rockwell Hardness values.

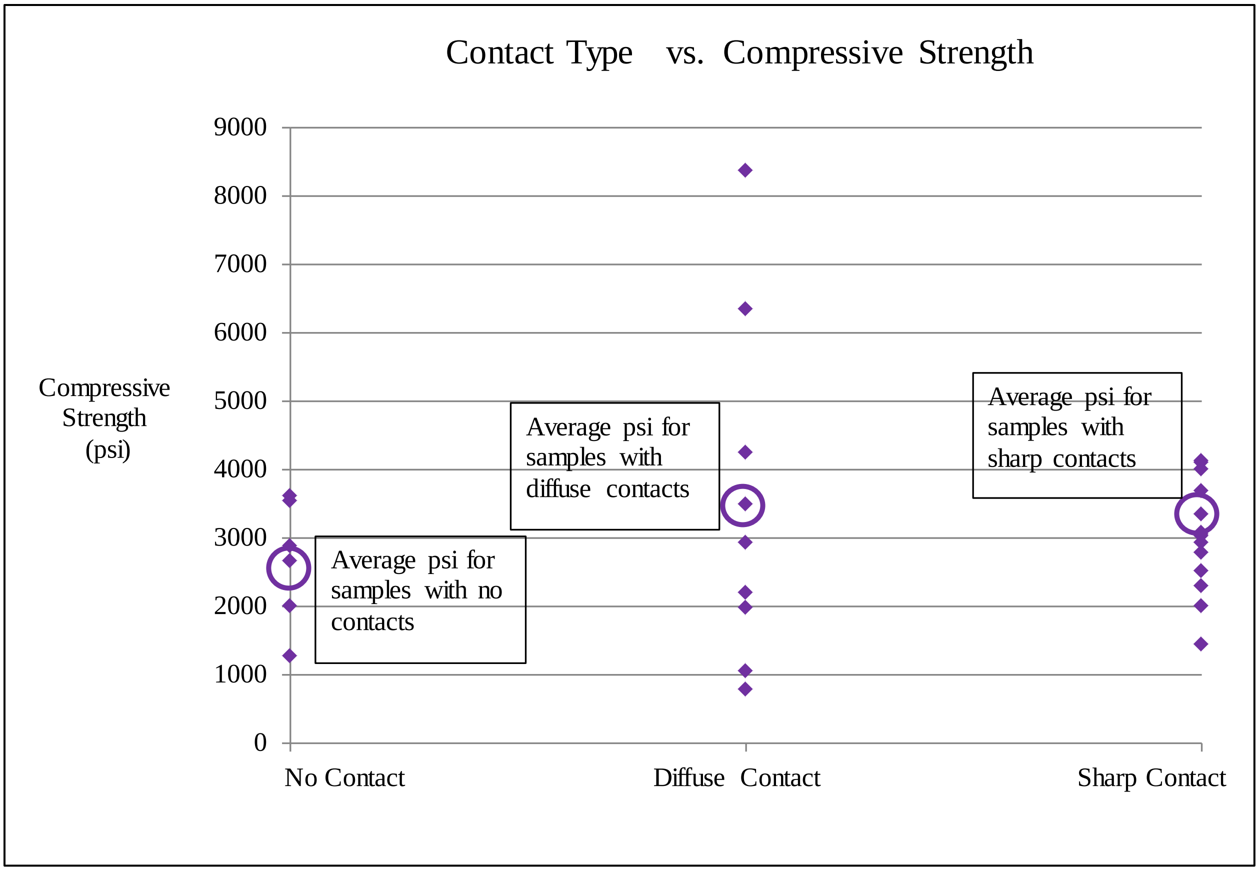

Figure 25. Compressive strength for samples with diffuse contacts have the highest average compressive strength and samples with no contacts have the lowest average compressive strength.

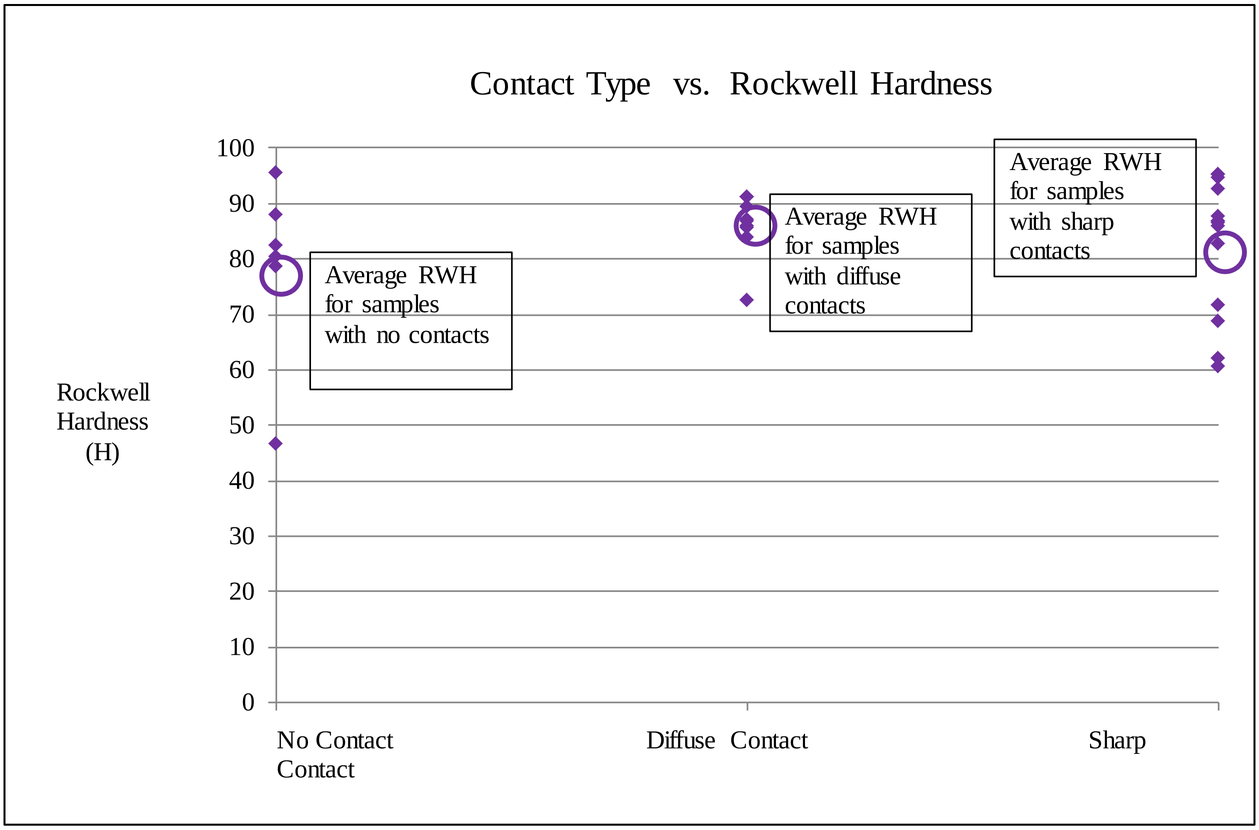

Figure 26. Samples with diffuse contacts have the highest average Rockwell Hardness value and samples with no contacts have the lowest average Rockwell Hardness value.

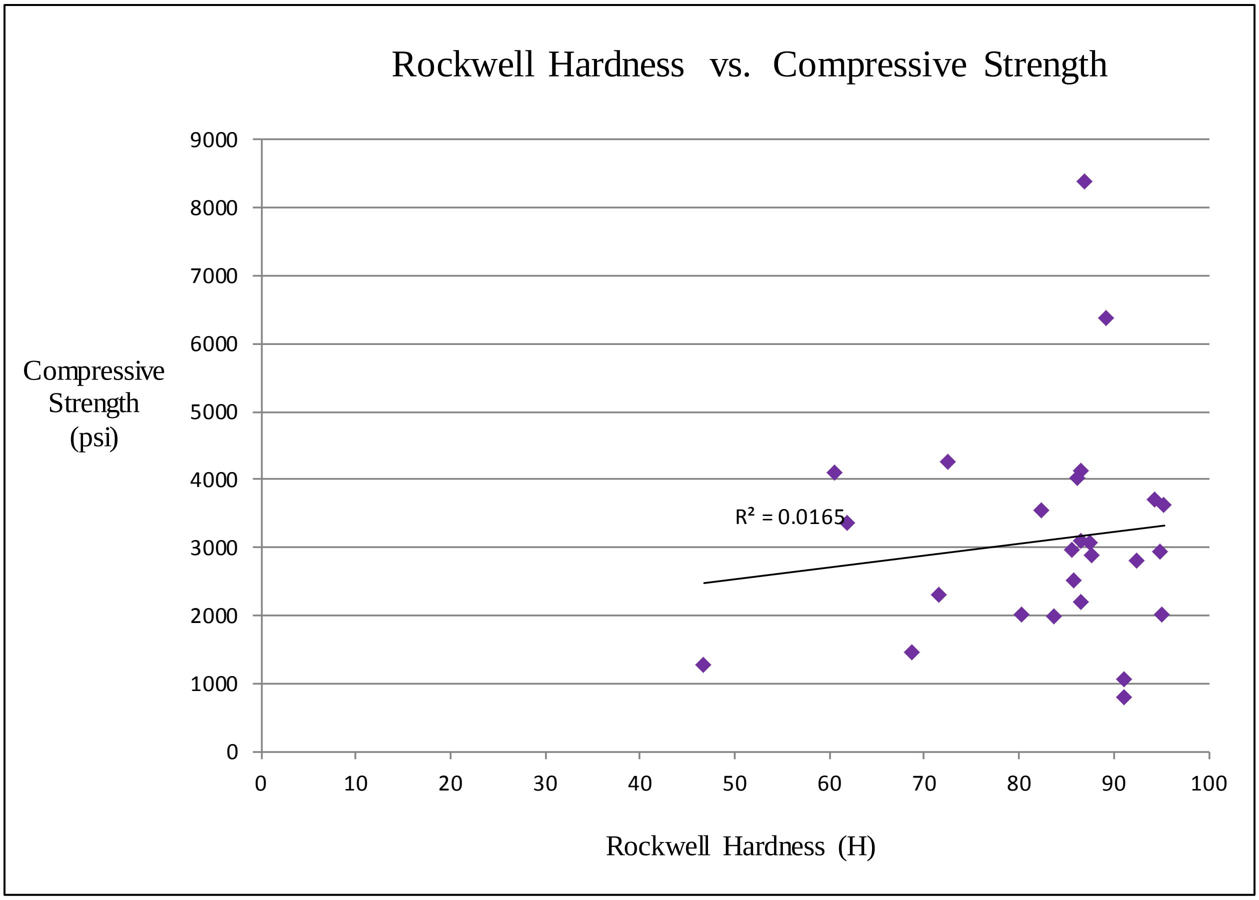

Figure 27. There is no correlation between Rockwell Hardness and compressive strength. Notice that the R^2 is close to 0.

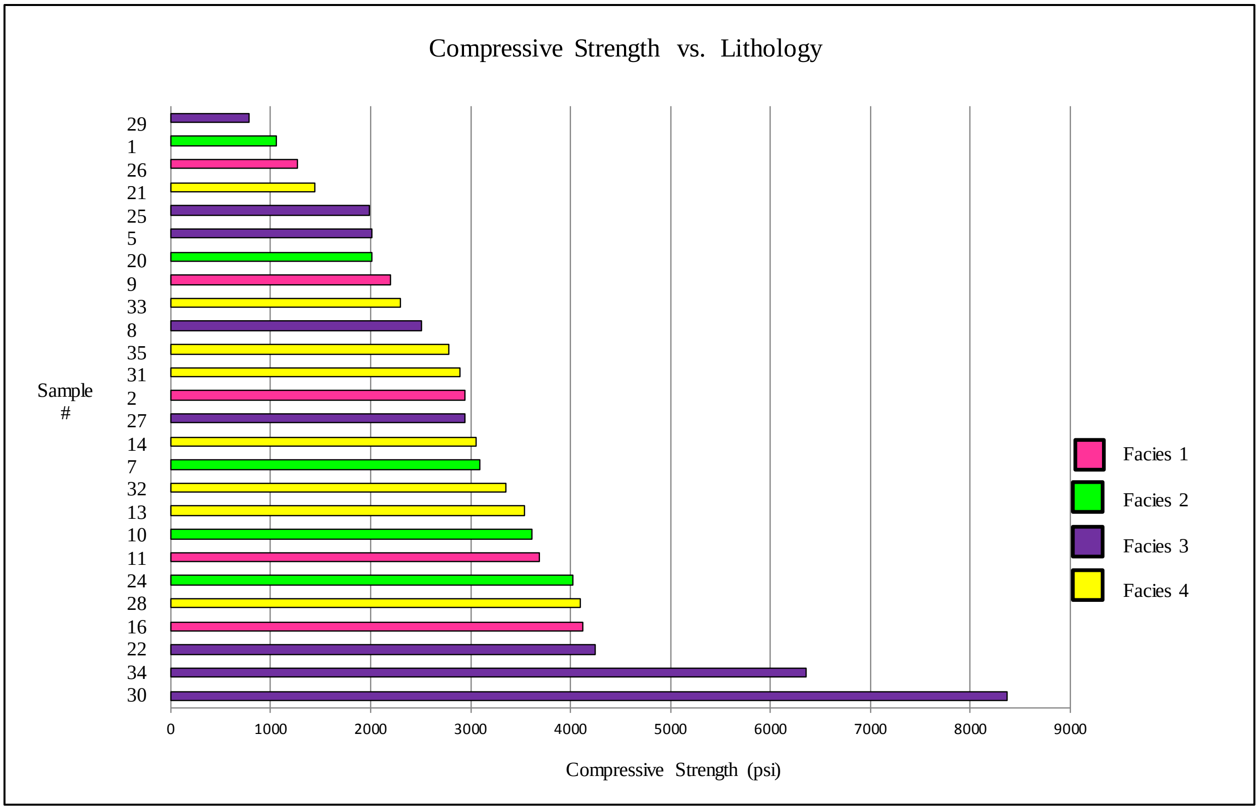

Figure 28. The strongest and weakest samples are both from Facies 3.

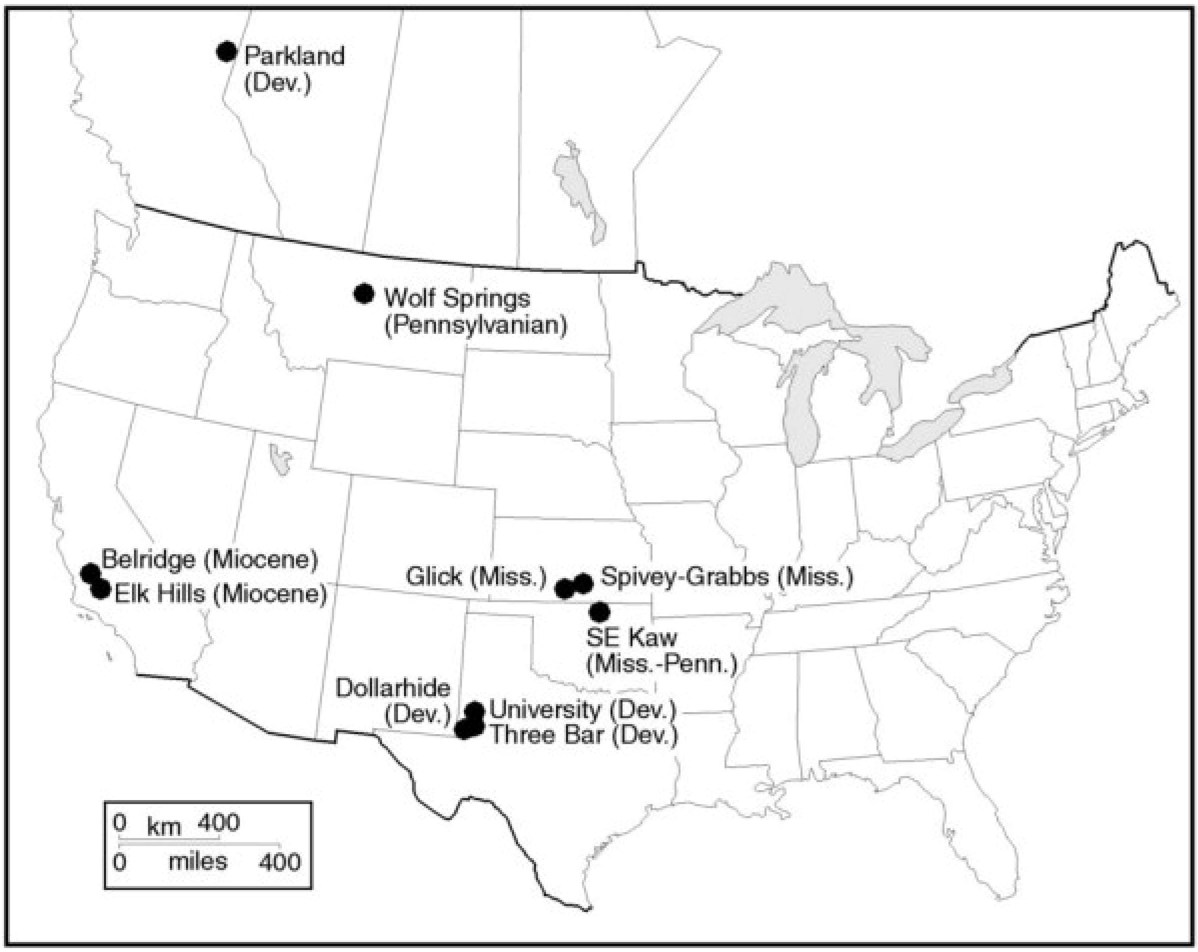

Figure 29. Rogers and Longman, 2001. Locations of Chert Reserviors in North America.

XII. APPENDIX


4D
5A 10
3A 13
2i 30
2K 25
5F 34
2B 14
2A
11


2H 32

2H

4A

iF 33

5E 31

3E 26
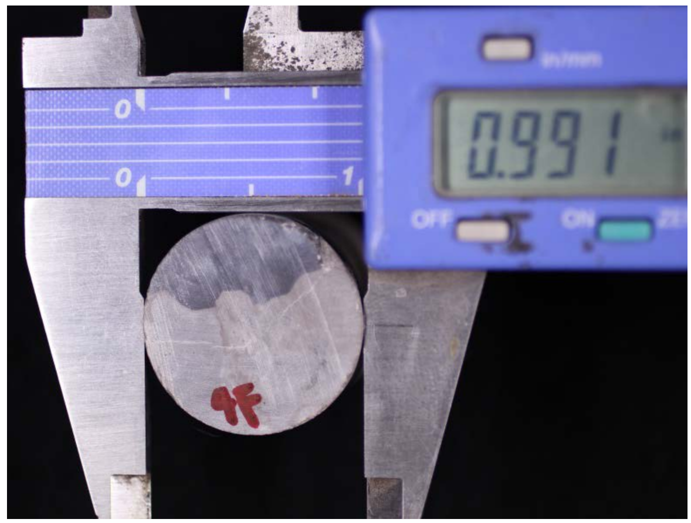
in/mm
0.991
OFF
ON
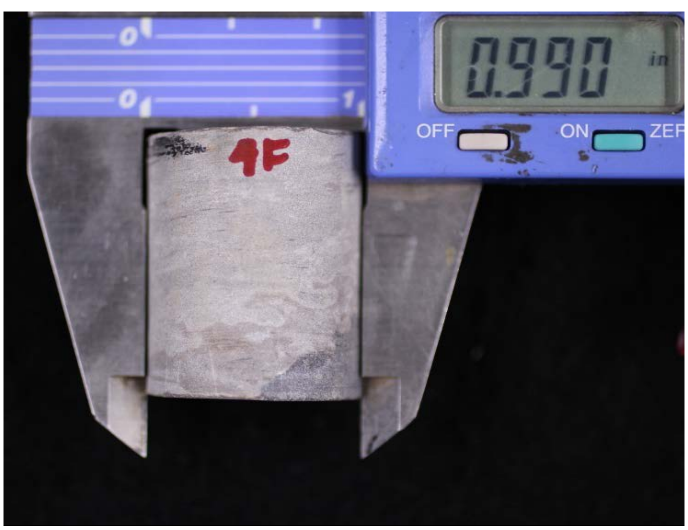
0.990
in
OFF
ON

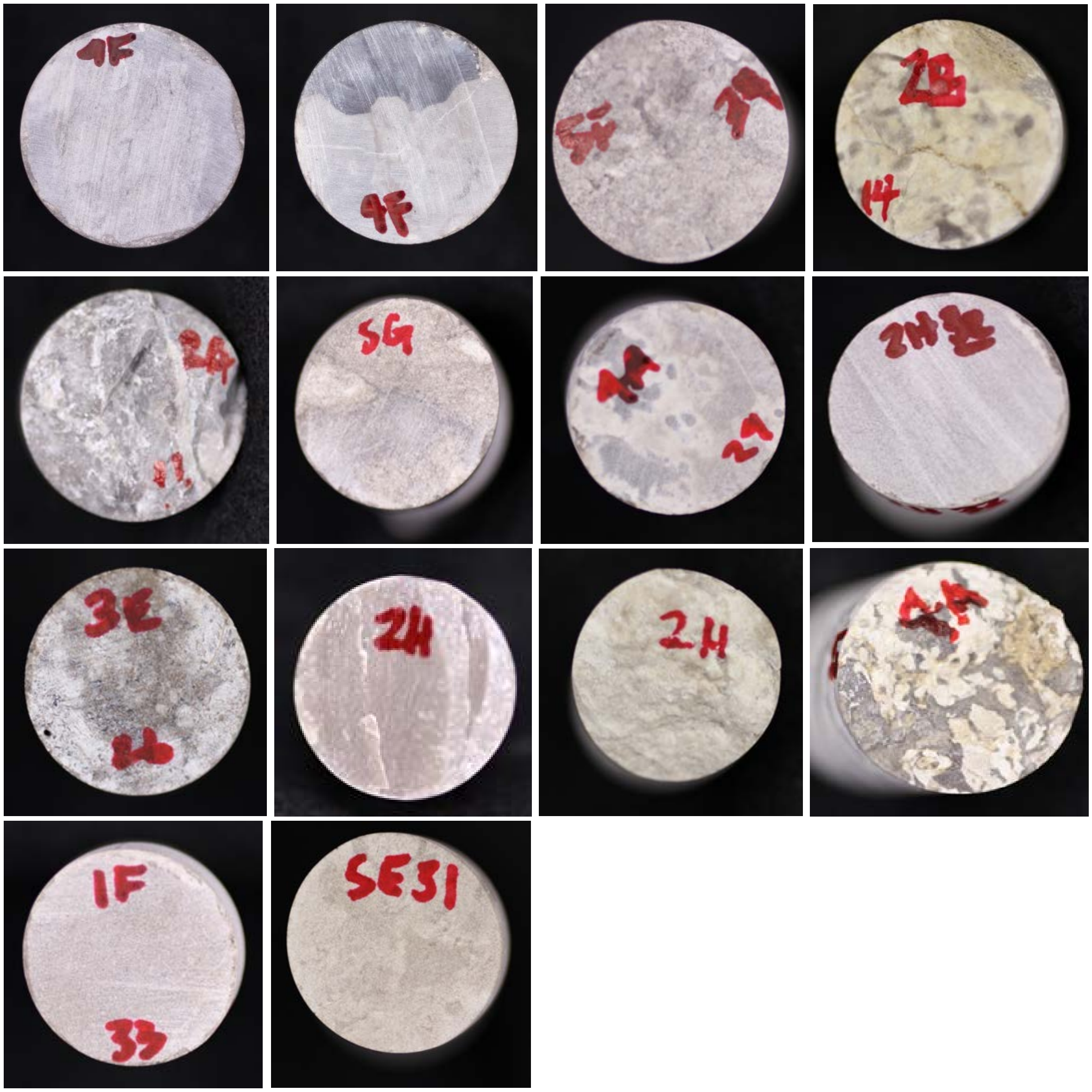

Photos of drilled plugs taken by Karen Buckland

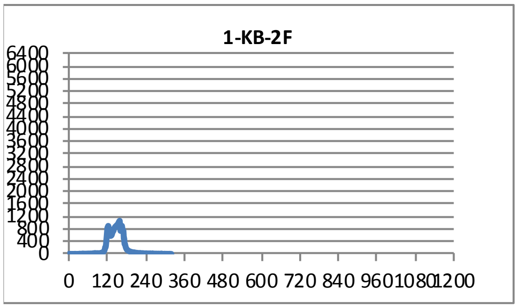
1-KB-2F
6400 6000 5600 5200 4800 4400 4000 3600 3200 2800 2400 2000 1600 1200 800 400 0
0 120 240 360 480 600 720 840 960 1080 1200

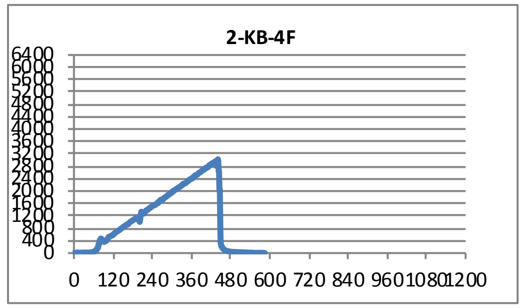
2-KB-4F
6400 6000 5600 5200 4800 4400 4000 3600 3200 2800 2400 2000 1600 1200 800 400 0
0 120 240 360 480 600 720 840 960 1080 1200

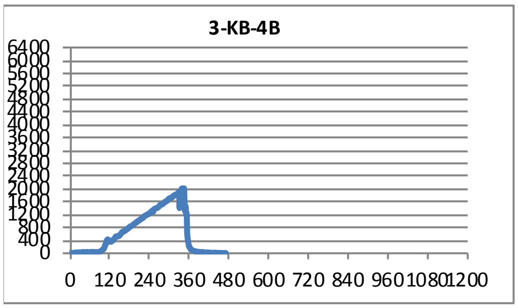
3-KB-4B
6400 6000 5600 5200 4800 4400 4000 3600 3200 2800 2400 2000 1600 1200 800 400 0
0 120 240 360 480 600 720 840 960 1080 1200

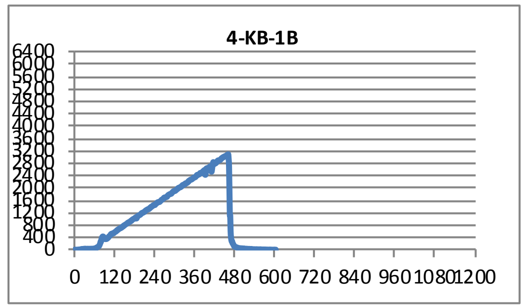
4-KB-1B
6400 6000 5600 5200 4800 4400 4000 3600 3200 2800 2400 2000 1600 1200 800 400 0
0 120 240 360 480 600 720 840 960 1080 1200

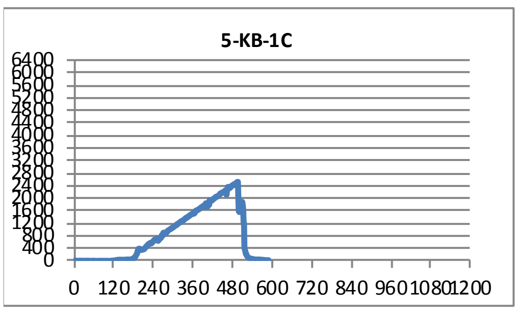
5-KB-1C
6400 6000 5600 5200 4800 4400 4000 3600 3200 2800 2400 2000 1600 1200 800 400 0
0 120 240 360 480 600 720 840 960 1080 1200

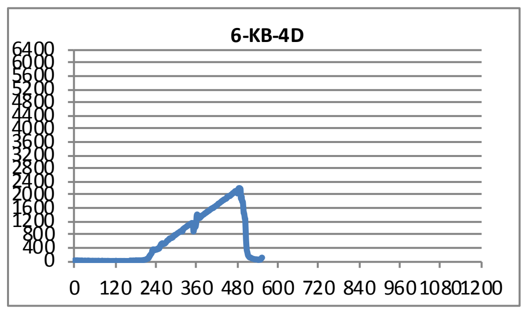
6-KB-4D
6400 6000 5600 5200 4800 4400 4000 3600 3200 2800 2400 2000 1600 1200 800 400 0
0 120 240 360 480 600 720 840 960 1080 1200

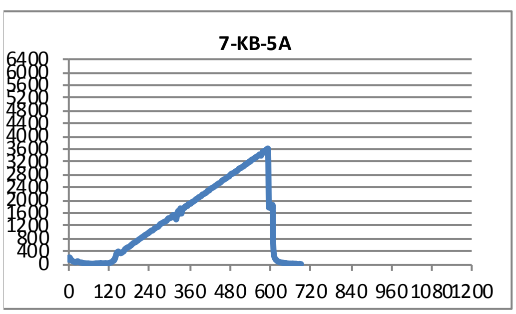
7-KB-5A
6400 6000 5600 5200 4800 4400 4000 3600 3200 2800 2400 2000 1600 1200 800 400 0
0 120 240 360 480 600 720 840 960 1080 1200

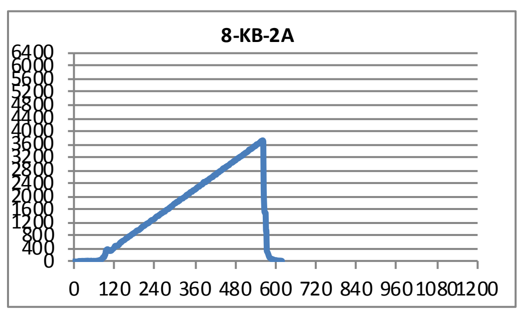
8-KB-2A
6400 6000 5600 5200 4800 4400 4000 3600 3200 2800 2400 2000 1600 1200 800 400 0
0 120 240 360 480 600 720 840 960 1080 1200

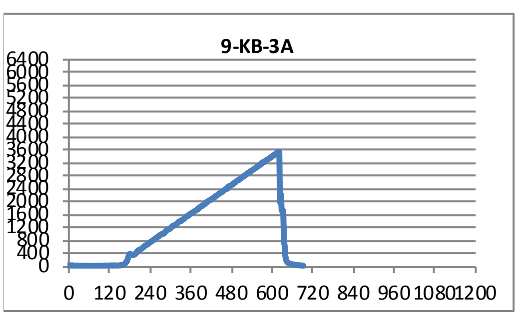
9-KB-3A
6400 6000 5600 5200 4800 4400 4000 3600 3200 2800 2400 2000 1600 1200 800 400 0
0 120 240 360 480 600 720 840 960 1080 1200

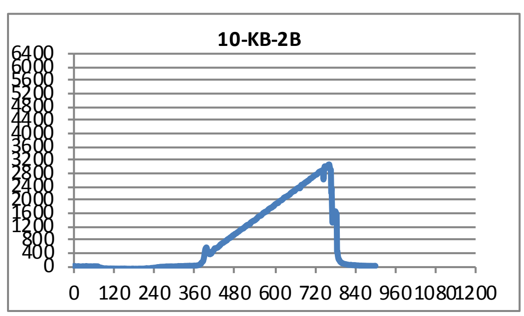
10-KB-2B
6400 6000 5600 5200 4800 4400 4000 3600 3200 2800 2400 2000 1600 1200 800 400 0
0 120 240 360 480 600 720 840 960 1080 1200

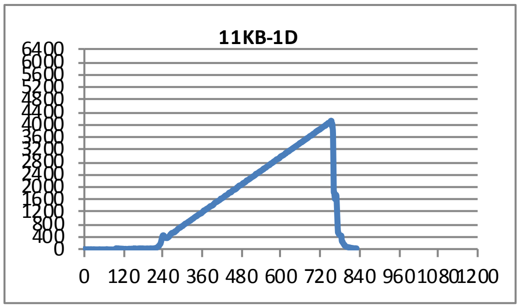
11KB-1D
6400 6000 5600 5200 4800 4400 4000 3600 3200 2800 2400 2000 1600 1200 800 400 0
0 120 240 360 480 600 720 840 960 1080 1200

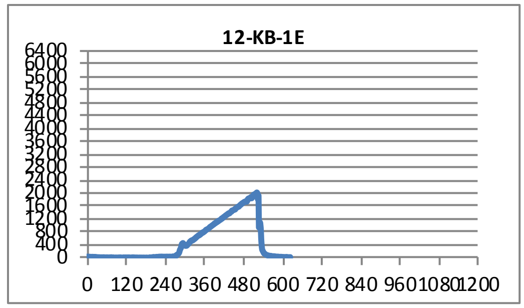
12-KB-1E
6400 6000 5600 5200 4800 4400 4000 3600 3200 2800 2400 2000 1600 1200 800 400 0
0 120 240 360 480 600 720 840 960 1080 1200

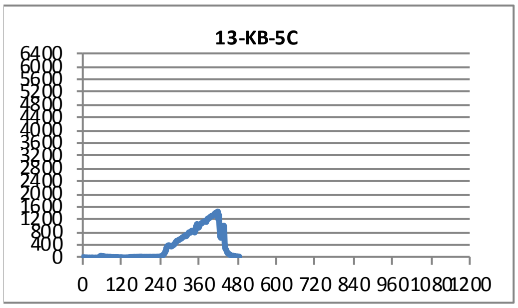
13-KB-5C
6400 6000 5600 5200 4800 4400 4000 3600 3200 2800 2400 2000 1600 1200 800 400 0
0 120 240 360 480 600 720 840 960 1080 1200

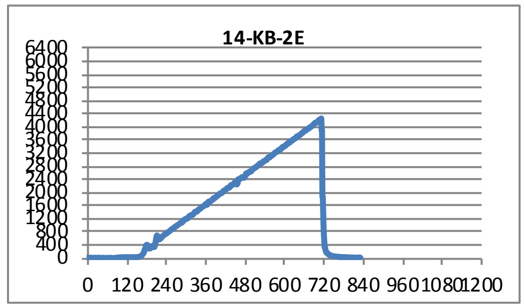
14-KB-2E
6400 6000 5600 5200 4800 4400 4000 3600 3200 2800 2400 2000 1600 1200 800 400 0
0 120 240 360 480 600 720 840 960 1080 1200

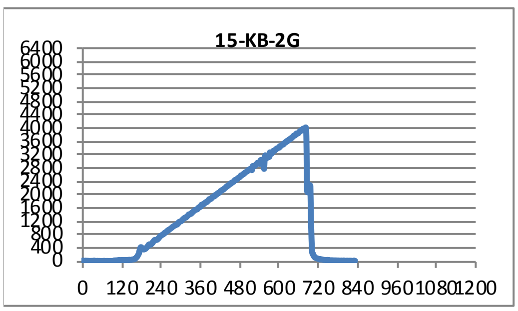
15-KB-2G
6400 6000 5600 5200 4800 4400 4000 3600 3200 2800 2400 2000 1600 1200 800 400 0
0 120 240 360 480 600 720 840 960 1080 1200

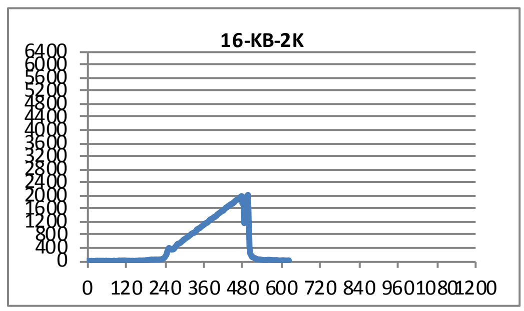
16-KB-2K
6400 6000 5600 5200 4800 4400 4000 3600 3200 2800 2400 2000 1600 1200 800 400 0
0 120 240 360 480 600 720 840 960 1080 1200

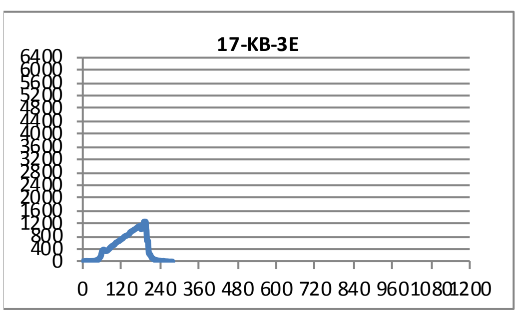
17-KB-3E
6400 6000 5600 5200 4800 4400 4000 3600 3200 2800 2400 2000 1600 1200 800 400 0
0 120 240 360 480 600 720 840 960 1080 1200

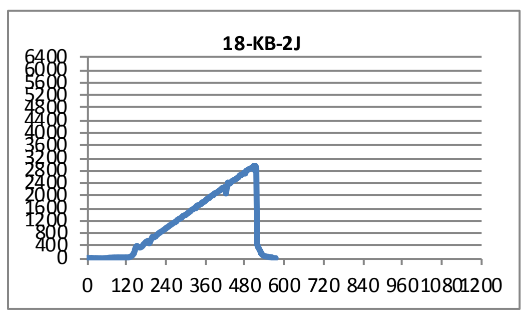
18-KB-2J
6400 6000 5600 5200 4800 4400 4000 3600 3200 2800 2400 2000 1600 1200 800 400 0
0 120 240 360 480 600 720 840 960 1080 1200

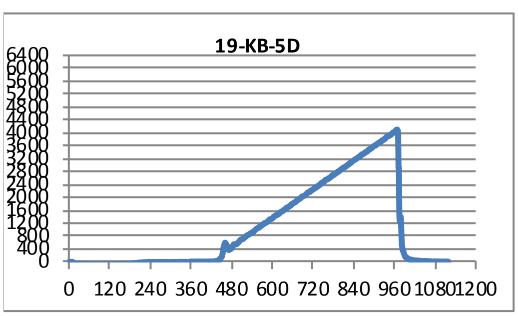
19-KB-5D
6400 6000 5600 5200 4800 4400 4000 3600 3200 2800 2400 2000 1600 1200 800 400 0
0 120 240 360 480 600 720 840 960 1080 1200

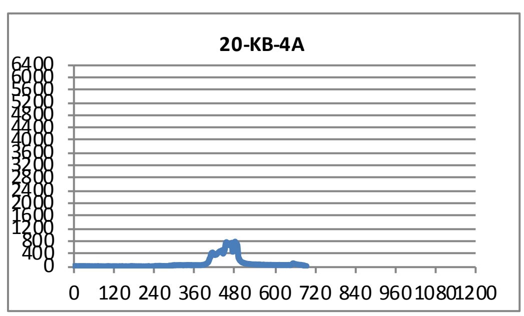
20-KB-4A
6400 6000 5600 5200 4800 4400 4000 3600 3200 2800 2400 2000 1600 1200 800 400 0
0 120 240 360 480 600 720 840 960 1080 1200

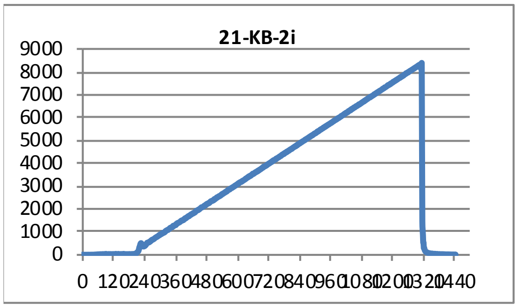

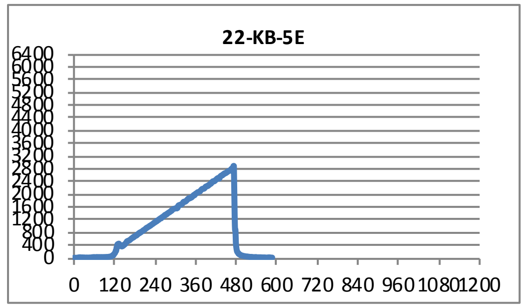

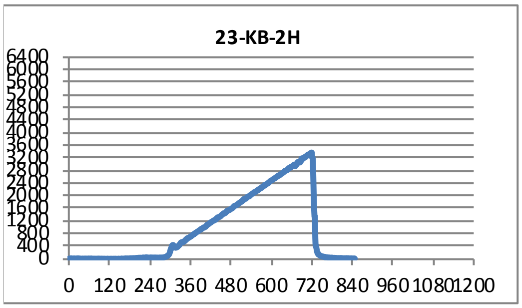

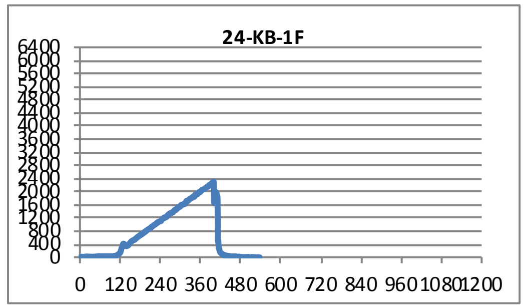

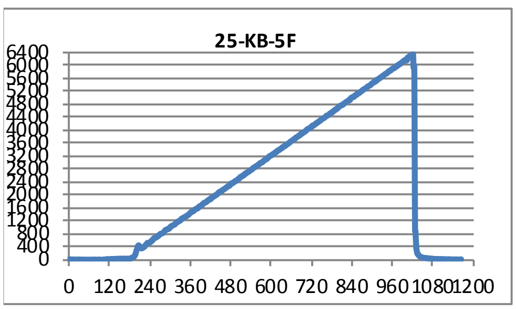

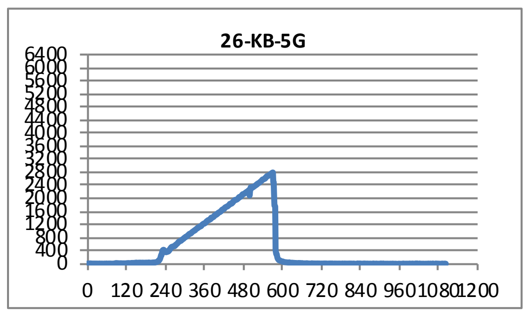

Tables of compressive strength tests

XIII. REFERENCES

Ameen, M.S., MacPherson, K., Al-Marhoon, M.I., Rahim, Z., 2012, Diverse Fracture Properties and Their Impact on Performance in Conventional and Tight-gas Reservoirs, Saudi Arabia: The Unayzah, South Haradh Case Study: AAPG Bulletin, vol. 96, no. 3, p. 459-492

Asszonyi, C., and Richter, R., 1979, The Continuum Theory of Rock Mechanics

ASTM International Designation: D 4543-08, Standard Practices for Preparing Rock Core as Cylindrical Test Specimens and Verifying Conformance to Dimensional Shape and Tolerances

ASTM International Designation: D 7012-10, Standard Test Method for Compressive Strength and Elastic Moduli of Intact Rock Core Specimens under Varying States of Stress and Temperatures

ASTM International Designation: E18-08b, Standard Test Methods for Rockwell Hardness of Metallic Materials

Blakey, R., 2009, Paleogeography and Geologic Evolution of North America: Images that Track the Ancient Landscapes of North America. http://jan.ucc.nau.edu/rcb7/nam.html

Dewhurst, D.N., Jones, R.M., 2003, Geomechanical, Microstructural, and Petrophysical Evolution in Experimentally Reactivated Cataclasites: Applications to Fault

Seal Prediction: Reply: AAPG Bulletin, v. 87, no. 10, p. 1684-1686

Dick, J.C., Shakoor, A., 1992, Lithological Controls of Mudrock Durability: Quarterly Journal of Engineering Geology, vol. 25, p. 31-46

Dreyer, W., 1973, The Science of Rock Mechanics

Durham, Louise, 2013, A New Old Horizontal Target, Mississippi Lime-A Thoughtful Challenge: AAPG Explorer, May 2013 edition, Accessed May 3, 2013, www.aapg.org

English, J. M., 2012, Thermomechanical Origin of Regional Fracture Systems: AAPG Bulliten, v.96, no. 9, p. 1597-1625

Fuenkajorn, K., Walsri, C. and PhueakphumIntrinsic, D., 2011, Variability of the Mechanical Properties of Maha Sarakham Salt: Quarterly Journal of Engineering Geology and Hydrogeology, vol. 44, p. 445–456

Goodman, R.E., 1980, Introduction to Rock Mechanics

Gutschick, R.C., and Sandberg, C.A., 1983, Mississippian Contenental Margins of the Conterminous United States: SEPM Special Publication No. 33, p. 79-96

Habib, P., 1983, An Outline of Soil and Rock Mechanics

Hennings, P., 2009, AAPG-SPE-SGE Hedberg Research Conference on "the Geologic Occurrence and Hydraulic Significance of Fractures in Reservoirs": AAPG Bulletin, v. 93, no. 11, p. 1407-1412

Hennings, P., Allwardt, P., Pijush, P., Zahm, C., Reid Jr., R., Alley, H., Kirschner, R., Lee, B., Hough, E., 2012, Relationship Between Fractures, Fault Zones, Stress, and Reservoir Productivity in the Suban Gas Field, Sumatra, Indonesia: AAPG Bulletin, vol. 96, no. 4, p. 753-772

Hudson, M., 2000, Coordinated Strike-Slip and Normal Faulting in the Southern Ozark Dome of Northern Arkansas: Deformation in Late Paleozoic Foreland: Geology, vol. 28, no. 6, p. 511-514

Hunt, L., Reynolds, S., Hadley, S., Downton, J., Chopra, S., 2011, Casual Fracture Prediction: Curvature, Stess, and Geomechanics: The Leading Edge, vol. 30, no. 11, p. 1274-1286

Laubach, S.E., Olson, J.E., Gross, M.R., 2009, Mechanical and Fracture Stratigraphy: AAPG Bulletin, v. 93, no. 11, p. 1413-1426

Luebking, G.A., Longman, M.W., Carlise, W.J., 2001, Unconformity-related Chert/Dolomite Production in the Pennsylvanian Amsden Formation, Wolf Springs Fields, Bull Mountains Basin of Central Montana: AAPG Bulletin, v. 85, no. 1, p. 131–148

Low, S.R., 2001, Rockwell Hardness Measurement of Metallic Materials: NIST Special Publication 960-5

Maerten, L., and Maerten, F., 2006, Chronologic Modeling of Faulted and Fractured Reservoirs Using Geomechanically Based Restoration: Technique and Industry Applications: AAPG Bulletin, vol. 90, no. 8, p. 1201-1226

Manger, W.L. and Evans, K.R., 2012, An Introduction to the Lower Mississippian (Kinderhookian-Osagean) Geology of the Tri-State Region, Southern Ozarks: A Guidebook Prepared for Atlas Resource Partners, L.P.

Mazzullo, S.J., Wilhite, B.W., Boardman, D.R., 2011, Lithostratigraphic Architecture of the Mississippian Reeds Spring Formation: Shale Shaker, The Journal of the Oklahoma Geological Society, vol. 61, no. 5, p. 254-269

(Middle Osagean) In Southwest Missouri, Northwest Arkansas, And Northeast

Oklahoma: Outcrop Analog Of Subsurface Petroleum Reservoirs

McFarland, J. D., (2004). Stratigraphic Summary of Arkansas, Information Circular 36, Arkansas Geological Survey, Little Rock, Arkansas, p. 37

Mickus, K. L., and Keller, G. R., (1992). Lithospheric structure of the south-central United States. Geology, vol. 20, no. 4, p. 335-338

Nadan, B. J., Engelder, T., 2009, Microcracks in New England Granitoids: A Record of Thermoelastic Relaxation During Exhumation of Intracontinental Crust: GSA Bulletin, vol. 121, no.1/2, p. 80-99

Olsen, J.E., Laubach, S.E., Lander, R.H., Natural Fracture Characterization in Tight Gas Sandstones: Integrating Mechanics and Diagenesis: AAPG Bulletin, vol. 93, no. 11, p. 1535-1549

Jeffrey J. Packard, J.J., Al-Aasm, I., Samson, I., Berger, Z., Davies, J., A Devonian Hydrothermal Chert Reservoir: The 225 bcf Parkland Field, British Columbia, Canada: AAPG Bulletin, v. 85, no. 1, p. 51–84

Pande, G.N., Beer, G., and Williams, J.R., 1990, Numerical Methods in Rock Mechanics

Pettitt, W., Pierce, M., Damjanac, B., Hazzard, J., Lorig, L., Fairhurst, C., Gil, I., Sanchez, M., Nagel, N., Reyes-Montes, J., Young, R.P., 2011, Fracture Network Engineering for Hydraulic Fracturing: The Leading Edge, vol. __, p. 844-853

Phillips, W.J., 1972, Hydraulic Fracturing and Minealization: Geological Society of London Journal, vol. 128, p. 337-359

Reid, S.A., McIntyre, J.L., 2001, Monterey Formation Porcelanite Reservoirs of the Elk Hills field, Kern County, California, AAPG Bulletin v. 85, no. 1, p. 169–189

Rogers, S., 2001, Deposition and Diagenesis of Mississippian Chat Reservoirs, North-Central Oklahoma: AAPG Bulletin, vol. 85, no. 1, p. 115-129

Rogers, J.P., Longman M.W., 2001, An Introduction to Chert Reservoirs of North America: AAPG Bulletin, vol. 85, no.1, p. 1-5

Ruppel, S.C., Barnaby, R.J., 2001, Contrasting Styles of Reservoir Development in Proximal and Distal Chert Facies: Devonian Thirtyone Formation, Texas: AAPG Bulletin, v. 85, no. 1, p. 7-33.

Ruppel, S.C., 2005, The Lower Devonian Thirtyone Formation of the Permian Basin: Dominance of Deep-Water, Siliceous Sedimentation: Bureau of Economic Geology

Sayers, C.M., Schutjens, P.M.T.M., 2007, An Introduction to Reservoir Geomechanics: The Leading Edge, vol. 26, p. 597-601

Sen, V., Settari, A., 2007, Stimulation of Permeability and Geomechanical Anisotropy in Fractured Reservoirs: The Leading Edge, vol. 26, p. 1128-1133

Settari, A., Sen, V., 2007, The Role of Geomechanics in Integrated Reservoir Modeling: The Leading Edge, vol. 26, p. 622-627

Slatt, R.M. and Abousleiman, Y., 2011, Merging Sequence Stratigraphy and Geomechanics for Unconventional Gas Shales: The Leading Edge, vol. 30, p. 274-282

Shelby, P.R., 1986, Depositional History of the St. Joe and Boone Formations in Northern Arkansas: Proceedings Arkansas Academy of Science, vol. XXXX, p. 67-71

Small, L., 1960, Hardness Theory and Practice

Smith, L.B., Read, J.F., 2000, Rapid Onset of Late Paleozoic Glaciation on Gondwana: Evidence from Upper Mississippian Strata of the Midcontinent, United States: Geology, vol. 28, no. 23, p. 279-282

Stoffell, B., Appold, M. S., Wilkinson, J.J, McClean, N.A., Jefferies, T.E., 2008, Geochemistry and Evolution of Mississippi Valley-Type Mineralizing Brines from the Tri-State and Northern Arkansas Districts Determined by LA-ICP-MS Microanalysis of Fluid Inclusions: Economic Geology, vol. 103, no. 7, p. 1411-1435

Sutherland, P. K, 1988, Late Mississippian and Pennsylvanian Depositional History in the Arkoma Basin Area, Oklahoma and Arkansas: GSA Bulletin, vol. 100, no. 11, p. 1787-1802

Szilágyi, K., ----, Hardness Studies on Porous Solids: Conference of Junior Researchers in Civil Engineering, p. 240-247

Watney, W., Guy, W., Byrnes, A., 2001, Characterization of the Mississippian chat in south-central Kansas: AAPG Bulletin, vol. 85, no. 1, p. 85-113

Willems, N., Easley, J.T., Rolfe, S.T., 1981, Strength of Materials